6

# Dynamic Simulation of Single and Combined Trajectory Path Generation and Control of A Seven Link Biped Robot

Ahmad Bagheri
*Peiman Naserredin Musavi*
*Guilan University*
*Iran*
*bagheri@guilan.ac.ir*

## 1. Introduction

Recently, numerous collaborations have been focused on biped robot walking pattern to trace the desired paths and perform the required tasks. In the current chapter, it has been focused on mathematical simulation of a seven link biped robot for two kinds of zero moment points (ZMP) including the Fixed and the Moving ZMP. In this method after determination of the breakpoints of the robot and with the aid of fitting a polynomial over the breakpoints, the trajectory paths of the robot will be generated and calculated. After calculation of the trajectory paths of the robot, the kinematic and dynamic parameters of the robot in Matlab environment and with respect to powerful mathematical functions of Matlab, will be obtained. The simulation process of the robot is included in the control process of the system. The control process contains Adaptive Method for known systems. The detailed relations and definitions can be found in the authors' published article [Musavi and Bagheri, 2007]. The simulation process will help to analyze the effects of drastic parameters of the robot over stability and optimum generation of the joint's driver actuator torques.

## 2. Kinematic of the robot

The kinematic of a seven link biped robot needs generation of trajectory paths of the robot with respect to certain times and locations in relevant with the assumed fixed coordinate system. In similarity of human and robot walking pattern, the process of path trajectory generation refers to determination of gait breakpoints. The breakpoints are determined and calculated with respect to system identity and conditions.
Afterward and in order to obtain comprehensive concept of the robot walking process, the following parameters and definitions will be used into the simulation process:
- Single Support phase: The robot is supported by one leg and the other is suspended in air
- Double support phase: The robot is supported by the both of its legs and the legs are in contact with the ground simultaneously
- $T_c$: Total traveling time including single and double support phase times.
- $T_d$: Double support phase time which is regarded as 20% of $T_c$



Source: Humanoid Robots, New Developments, Book edited by: Armando Carlos de Pina Filho
ISBN 978-3-902613-02-8, pp.582, I-Tech, Vienna, Austria, June 2007

- $T_m$ : The time which ankle joint has reached to its maximum height during walking cycle.

: Step number $k$ -

Ankle joint maximum height: $H_{ao}$ -

- $L_{ao}$ : The horizontal traveled distance between ankle joint and start point when the ankle joint has reached to its maximum height.

Step length: $D_s$ -

: Foot lift angle and contact angle with the level ground $q_b, q_f$ -

- $\lambda$ : Surface slope

- $h_s$ : Stair level height-

- $H_{st}$ : Foot maximum height from stair level

- $x_{ed}$ : The horizontal distance between hip joint and the support foot (Fixed coordinate system) at the start of double support phase time.

- $x_{sd}$ : The horizontal distance between hip joint and the support foot (Fixed coordinate system) at the end of double support phase time.

- F. C. S: The fixed coordinate system which would be supposed on support foot in each step.

-M.C : The mass centers of the links

- Saggital plane: The plane that divides the body into right and left sections.

- Frontal plane: The plane parallel to the long axis of the body and perpendicular to the saggital plane.

The saggital and frontal planes of the human body are shown in figure (1.1) where the transverse plane schematic and definition have been neglected due to out of range of our calculation domain.

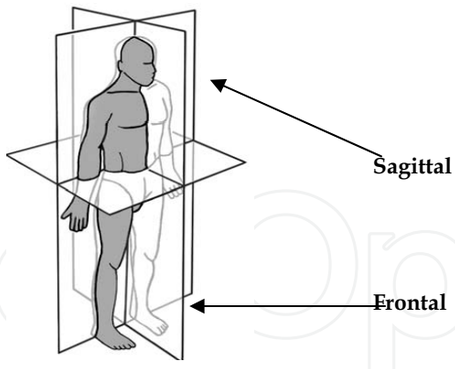


Fig. (1.1). The body configuration with respect to various surfaces.

The main role for the optimum trajectory path generation must be imagined upon hip and ankle joints of the robot. On the other hand, with creating smooth paths of the joints and with the aid of the breakpoints, the robot can move softly with its optimum movement parameters such as minimum actuator torques of joints (Shank) including integrity of the joints kinematic parameters.

The important parameters of the robot can be assumed as the listed above and are shown in figures (1.2) and (1.3).

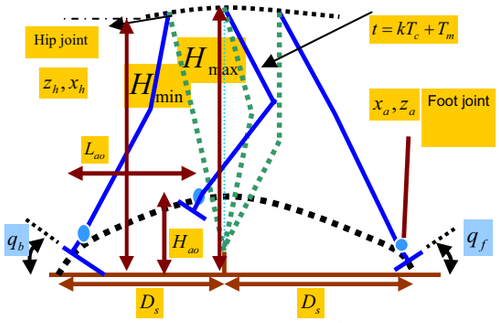


Fig. (1.2). The robot important parameters for calculation of trajectory path of a seven link biped robot.

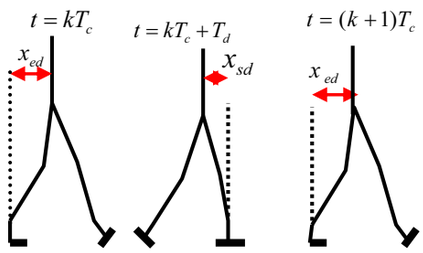


Fig. (1.3). The variables of hip: $x_{ed}, x_{sd}$.

With respect to saggital investigation of the robot, the most affecting parameters of the mentioned joints can be summarized as below:

1) **Hip joint**
2) **Ankle joint**

Obviously, the kinematic and dynamic attitude of shank joint will be under influence of the both of above mentioned joints. As can be seen from figure (1.2), the horizontal and vertical components of the joints play a great role in trajectory paths generation. This means that timing-process and location of the joints with respect to the fixed coordinate system which would be supposed on the support foot have considerable effects on the smooth paths and subsequently over stability of the robot. Regarding the above expressions and conditions, the vertical and horizontal components of the joints can be categorized and calculated as the following procedure. With respect to the conditions of the surfaces and figure (1.2) and (1.3), the components are classified as below:

### 2.1) Foot angle on horizontal surface or stair

$$\theta_a(t) = \begin{cases} -q_{gs} & t = kT_c \\ -q_b & t = kT_c + T_d \\ q_f & t = (k+1)T_c \\ q_{gf} & t = (k+1)T_c + T_d \end{cases} \quad (1)$$

### 2.2) Foot angle on declined surfaces

$$\theta_a(t)=\begin{cases}(\lambda+q_{gs}) & t=kT_c\\ \lambda-q_b & t=kT_c+T_d\\ \lambda+q_f & t=(k+1)T_c\\ \lambda+q_{gf} & t=(k+1)T_c+T_d\end{cases} \tag{2}$$

### 2.3) The displacements of Horizontal and Vertical Foot Traveling Over Horizontal Surface or Stair

With respect to figures (1.2) and (1.3), the horizontal and vertical components of ankle joint can be shown as below:

$$x_{ahor}(t)=\begin{cases}kD_s & t=kT_c\\ kD_s+l_{an}\sin q_b+\cdots & t=kT_c+T_d\\ l_{af}(1-\cos q_b) & \\ kD_s+L_{ao} & t=kT_c+T_m\\ (k+2)D_s-l_{an}\sin q_f-\cdots & t=(k+1)T_c\\ l_{ab}(1-\cos q_f) & \\ (k+2)D_s & t=(k+1)T_c+T_d\end{cases} \tag{3}$$

$$z_{ahor}(t)=\begin{cases}h_{gs}+l_{an} & t=kT_c\\ h_{gs}+l_{af}\sin q_b+l_{an}\cos q_b & t=kT_c+T_d\\ H_{ao} & t=kT_c+T_m\\ h_{ge}+l_{ab}\sin q_f+l_{an}\cos q_f & t=(k+1)T_c\\ h_{ge}+l_{an} & t=(k+1)T_c+T_d\end{cases} \tag{4}$$

$$z_{stair}(t)=\begin{cases}(k-1)h_{st}+l_{an} & t=kT_c\\ (k-1)h_{st}+l_{af}\sin q_b+\cdots & t=kT_c+T_d\\ l_{an}\cos q_b & \\ kh_{st}+H_{st} & t=kT_c+T_m\\ (k+1)h_{st}+l_{ab}\sin q_f+\cdots & t=(k+1)T_c\\ l_{an}\cos q_f & \\ (k+1)h_{st}+l_{an} & t=(k+1)T_c+T_d\end{cases} \tag{5}$$

### 2.4) The displacements of Horizontal and Vertical Foot Traveling Over declined Surface

$$x_{a,dec}(t)=\begin{cases}kD_s\cos\lambda-l_{an}\sin\lambda & t=kT_c\\ (kD_s+l_{af})\cos\lambda+\cdots & t=kT_c+T_d\\ l_{an}\sin(q_b-\lambda)-l_{af}\cos(q_b-\lambda) & \\ (kD_s+L_{ao})\cos\lambda & t=kT_c+T_m\\ ((k+2)D_s-l_{ab})\cos\lambda-\cdots & t=(k+1)T_c\\ l_{an}\sin(q_f+\lambda)+l_{ab}\cos(q_f+\lambda) & \\ (k+2)D_s\cos\lambda-l_{an}\sin\lambda & t=(k+1)T_c+T_d\end{cases} \tag{6}$$

$$z_{a,dec}(t)=\begin{cases} kD_s\sin\lambda+l_{an}\cos\lambda & t=kT_c \\ (kD_s+l_{af})\sin\lambda+\cdots & t=kT_c+T_d \\ +l_{an}\cos(q_b-\lambda)+l_{af}\sin(q_b-\lambda) & \\ (kD_s+L_{ao})\sin\lambda+H_{ao}\cos\lambda & t=kT_c+T_m \\ ((k+2)D_s-l_{ab})\sin\lambda+\cdots & t=(k+1)T_c \\ l_{an}\sin(q_f+\lambda)+l_{ab}\cos(\pi/2-(q_f+\lambda)) & \\ (k+2)D_s\sin\lambda+l_{an}\cos\lambda & t=(k+1)T_c+T_d \end{cases} \quad (7)$$

Assuming the above expressed breakpoints and also applying the following boundary condition of the robot during walking cycle, generation of the ankle joint trajectory path can be performed. The boundary conditions of the definite system are determined with respect to physical and geometrical specifications during movement of the system. As can be seen from figure (1.2) and (1.3), the linear and angular velocity of foot at the start and the end of double support phase equal to zero:

$$\begin{cases} \dot{\theta}_a(kT_c)=0 \\ \dot{\theta}_a((k+1)T_c+T_d)=0 \end{cases}$$
$$\begin{cases} \dot{x}_a(kT_c)=0 \\ \dot{x}_a((k+1)T_c+T_d)=0 \end{cases} \quad (8)$$
$$\begin{cases} \dot{z}_a(kT_c)=0 \\ \dot{z}_a((k+1)T_c+T_d)=0 \end{cases}$$

The best method for generation of path trajectories refers to mathematical interpolation. There are several cases for obtaining the paths with respect to various conditions of the movement such as number of breakpoints and boundary conditions of the system. Regarding the mentioned conditions of a seven link biped robot, Spline and Vandermonde Matrix methods seem more suitable than the other cases of interpolation process. The Vandermonde case is the simplest method with respect to calculation process while it will include calculation errors with increment of breakpoint numbers. The stated defect will not emerge on Spline method and it will fit the optimum curve over the breakpoints regardless the number of points and boundary conditions. With respect to low number of domain breakpoints and boundary conditions of a seven link biped robot, there are no considerable differences in calculation process of Vandermonde and Spline methods. For an example, with choosing one of the stated methods and for relations (7) and (8), a sixth-order polynomial or third-order spline can be fitted for generation of the vertical movement of ankle joint.

### 2.5) Hip Trajectory Interpolation for the Level Ground [Huang and et. Al, 2001] and Declined Surfaces

From figures (1.2) and (1.3), the vertical and horizontal displacements of hip joint can be written as below:

$$x_{\substack{h,Hor,\\ stair}}=\begin{cases} kD_s+x_{ed} & t=kT_c \\ (k+1)D_s-x_{sd} & t=kT_c+T_d \\ (k+1)D_s+x_{ed} & t=(k+1)T_c \end{cases} \quad (9)$$

$$x_{h,Dec.}=\begin{cases}(kD_s+x_{ed})\cos\lambda & t=kT_c\\ ((k+1)D_s-x_{sd})\cos\lambda & t=kT_c+T_d\\ ((k+1)D_s+x_{ed})\cos\lambda & t=(k+1)T_c\end{cases} \tag{10}$$

$$z_{h,Hor.}=\begin{cases}H_{h\min} & t=kT_c\\ H_{h\max} & t=kT_c+.5(T_c-T_d)\\ H_{h\min} & t=(k+1)T_c\end{cases} \tag{11}$$

$$z_{h,Dec.}\quad \begin{array}{l} H_{h\min}\cos\lambda \quad \cdots, t \quad kT_c \\ (kD_s \quad x_{ed})\sin\lambda \\ H_{h\max}\cos\lambda \quad \cdots, t \quad kT_c \quad .5(T_c \quad T_d) \\ \quad (kD_s \quad x_{sd})\sin\lambda \\ H_{h\min}\cos\lambda \quad \cdots, \ t \quad (k \quad 1)T_c \\ ((k \quad 1)D_s \quad x_{ed})\sin\lambda, \end{array} \tag{12}$$

$$z_{stair}=\begin{cases}(k-1)h_s+H_{h\min} & t=kT_c\\ kh_s+H_{h\max} & t=kT_c+.5(T_c-T_d)\\ kh_s+H_{h\min} & t=(k+1)T_c\end{cases} \tag{13}$$

Where, in the above expressed relations, $H_{\min}$ and $H_{\max}$ indicate the minimum and maximum height of hip joint from the fixed coordinate system. Obviously and with respect to figure (1.2), the ankle and hip joint parameters including $x_a, z_a$ and $x_h, z_h$ play main role in optimum generation of the trajectory paths of the robot. With utilization of relations (1)-(13) and using the mathematical interpolation process, the trajectory paths of the robot will be completed.

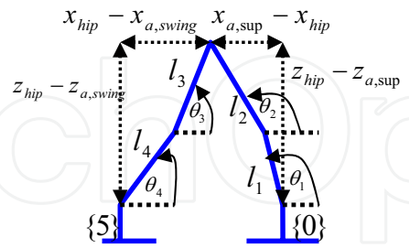


Fig. (1.4). The link's angles and configurations.

Regarding figure (1.4) and the trajectory paths generation of the robot based on four important parameters of the system ($x_a, z_a$ and $x_h, z_h$), the first kinematic parameter of the robot can be obtained easily. On the other hand, with utilization of inverse kinematics, the link's angle of

the robot will be calculated with respect to the domain nonlinear mathematical equations. As can be seen from figure (1.4), the equations can be written as below:

$$l_1 \cos(\pi-\theta_1)+l_2 \cos(\pi-\theta_2)=a$$
$$l_1 \sin(\pi-\theta_1)+l_2 \sin(\pi-\theta_2)=b \quad (14)$$
$$l_3 \cos(\theta_3)+l_4 \cos(\theta_4)=c \quad (15)$$
$$l_3 \sin(\theta_3)+l_4 \sin(\theta_4)=d$$

Where,

$a = x_{a,Sup} - x_{hip}$

$b = z_{hip} - z_{a,Sup}$

$c = x_{hip} - x_{a,swing}$

$d = z_{hip} - z_{a,swing}$

The all of conditions and the needed factors for solving of the relations (14) and (15) have been provided. The right hand of relations (14) and (15) are calculated from the interpolation process. For the stated purpose and with beginning to design program in MALAB environment and with utilization of strong commands such as **fsolve**, the angles of the links are calculated numerically. In follow and using kinematic chain of the robot links, the angular velocity and acceleration of the links and subsequently the linear velocities and accelerations are obtained. With respect to figure (1.5) and assuming the unit vectors parallel to the link's axis and then calculation of the link's position vectors relative to the assumed F.C.S, the following relations are obtained:

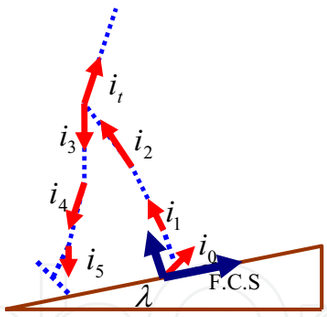


Fig. (1.5). The assumed unit vectors to obtain the position vectors.

$$\vec{r}_0 = l_{m.c}(\cos(\beta_{m.c}+q_f)I+\sin(\beta_{m.c}+q_f)K) \quad (16)$$

$$\vec{r}_1 = (l_0 \cos(\beta_{tot}+q_f)+l_{c1}\cos(\theta_1-\lambda))I + (l_{c1}\sin(\theta_1-\lambda)+l_0 \sin(\beta_{tot}+q_f))K \quad (17)$$

$$\vec{r}_2 = (l_0 \cos(\beta_{tot}+q_f)+l_1\cos(\theta_1-\lambda) - l_{c2}\cos(\pi-\theta_2+\lambda))I + (l_1 \sin(\theta_1-\lambda) + l_0 \sin(\beta_{tot}+q_f)+l_{c2}\sin(\pi-\theta_2+\lambda))K \quad (18)$$

$$\begin{aligned}\vec{r}_3 &= (l_0\cos(\beta_{tot}+q_f)+l_1\cos(\theta_1-\lambda)\\ &-l_2\cos(\pi-\theta_2+\lambda)-l_{c3}\cos(\theta_3-\lambda))I\\ &+(l_1\sin(\theta_1-\lambda)+l_0\sin(\beta_{tot}+q_f)\\ &+l_2\sin(\pi-\theta_2+\lambda)-l_{c3}\sin(\theta_3-\lambda))K\end{aligned} \tag{19}$$

$$\begin{aligned}\vec{r}_4 &= (l_0\cos(\beta_{tot}+q_f)+l_1\cos(\theta_1-\lambda)\\ &-l_2\cos(\pi-\theta_2+\lambda)-l_3\cos(\theta_3-\lambda)\\ &-l_{c4}\cos(\theta_4-\lambda))I+(l_1\sin(\theta_1-\lambda)\\ &+l_0\sin(\beta_{tot}+q_f)+l_2\sin(\pi-\theta_2+\lambda)\\ &-l_3\sin(\theta_3-\lambda)-l_{c4}\sin(\theta_4-\lambda))K\end{aligned} \tag{20}$$

$$\begin{aligned}\vec{r}_5 &= (l_0\cos(\beta_{tot}+q_f)+l_1\cos(\theta_1-\lambda)\\ &-l_2\cos(\pi-\theta_2+\lambda)-l_3\cos(\theta_3-\lambda)\\ &-l_4\cos(\theta_4-\lambda)-l_{5m.c}\cos(\pi/2-\lambda+\beta_{s,m.s}-q_b))I\\ &+(l_1\sin(\theta_1-\lambda)+l_0\sin(\beta_{tot}+q_f)\\ &+l_2\sin(\pi-\theta_2+\lambda)-l_3\sin(\theta_3-\lambda)\\ &-l_4\sin(\theta_4-\lambda)-l_{5m.c}\sin(\pi/2-\lambda+\beta_{s,m.s}-q_b)))K\end{aligned} \tag{21}$$

$$\begin{aligned}\vec{r}_{tor} &= (l_0\cos(\beta_{tot}+q_f)+l_1\cos(\theta_1-\lambda)\\ &-l_2\cos(\pi-\theta_2+\lambda)+l_{tor}\cos(\pi/2-\theta_{tor}-\lambda))I\\ &+(l_1\sin(\theta_1-\lambda)+l_0\sin(\beta_{tot}+q_f)\\ &+l_2\sin(\pi-\theta_2+\lambda)+l_{tor}\sin(\pi/2-\theta_{tor}-\lambda))K\end{aligned} \tag{22}$$

As can be seen from relations (16)-(22), the all of position vectors have been calculated with respect to F.C.S for inserting into ZMP formula. The ZMP concept will be discussed in the next sub-section. Now, with the aid of first and second differentiating of relation (16)-(22), the linear velocities and accelerations of the link's mass centers can be calculated within relations (23)-(29).

$$\vec{v}_0 = l_{m.c}\vec{\omega}_0(-\sin(\beta_{m.c}+q_f)I+\cos(\beta_{m.c}+q_f)K) \tag{23}$$

$$\begin{aligned}\vec{v}_1 &= (-l_0\vec{\omega}_0\sin(\beta_{tot}+q_f)-l_{c1}\vec{\omega}_1\sin(\theta_1-\lambda))I\\ &+(l_{c1}\vec{\omega}_1\cos(\theta_1-\lambda)+l_0\cos(\beta_{tot}+q_f))K\end{aligned} \tag{24}$$

$$\begin{aligned}\vec{v}_2 &= (-l_0\vec{\omega}_0\sin(\beta_{tot}+q_f)-l_1\vec{\omega}_1\sin(\theta_1-\lambda)\\ &-l_{c2}\vec{\omega}_2\sin(\pi-\theta_2+\lambda))I+(l_1\vec{\omega}_1\cos(\theta_1-\lambda)\\ &+l_0\vec{\omega}_0\cos(\beta_{tot}+q_f)-l_{c2}\vec{\omega}_2\cos(\pi-\theta_2+\lambda))K\end{aligned} \tag{25}$$

$$\begin{aligned}\vec{v}_3 &= (-l_0\vec{\omega}_0\sin(\beta_{tot}+q_f)-l_1\vec{\omega}_1\sin(\theta_1-\lambda)\\ &-l_2\vec{\omega}_2\sin(\pi-\theta_2+\lambda)+l_{c3}\vec{\omega}_3\sin(\theta_3-\lambda))I\\ &+(l_1\vec{\omega}_1\cos(\theta_1-\lambda)+l_0\vec{\omega}_0\cos(\beta_{tot}+q_f)\\ &-l_2\vec{\omega}_2\cos(\pi-\theta_2+\lambda)-l_{c3}\vec{\omega}_3\cos(\theta_3-\lambda))K\end{aligned} \tag{26}$$

$$\begin{aligned}\vec{v}_4 &= (-l_0\vec{\omega}_0\sin(\beta_{tot}+q_f)-l_1\vec{\omega}_1\sin(\theta_1-\lambda)\\ &-l_2\vec{\omega}_2\sin(\pi-\theta_2+\lambda)+l_3\vec{\omega}_3\sin(\theta_3-\lambda)\\ &+l_{c4}\vec{\omega}_4\sin(\theta_4-\lambda))I+(l_1\vec{\omega}_1\cos(\theta_1-\lambda)\\ &+l_0\vec{\omega}_0\cos(\beta_{tot}+q_f)-l_2\vec{\omega}_2\cos(\pi-\theta_2+\lambda)-\\ &l_3\vec{\omega}_3\cos(\theta_3-\lambda)-l_{c4}\vec{\omega}_4\cos(\theta_4-\lambda))K\end{aligned} \tag{27}$$

$$\begin{aligned}\vec{v}_5 &= (-l_0\vec{\omega}_0\sin(\beta_{tot}+q_f)-l_1\vec{\omega}_1\sin(\theta_1-\lambda)\\ &-l_2\vec{\omega}_2\sin(\pi-\theta_2+\lambda)+l_3\vec{\omega}_3\sin(\theta_3-\lambda)\\ &+l_4\vec{\omega}_4\sin(\theta_4-\lambda)-l_{5mc}\vec{\omega}_5\sin(\pi/2-\lambda+\beta_{s,mc}-q_b))I\\ &+(l_1\vec{\omega}_1\cos(\theta_1-\lambda)+l_0\vec{\omega}_0\cos(\beta_{tot}+q_f)\\ &-l_2\vec{\omega}_2\cos(\pi-\theta_2+\lambda)-l_3\vec{\omega}_3\cos(\theta_3-\lambda)\\ &-l_4\vec{\omega}_4\cos(\theta_4-\lambda)+l_{5mc}\vec{\omega}_5\cos(\pi/2-\lambda+\beta_{s,mc}-q_b))K\end{aligned} \tag{28}$$

$$\begin{aligned}\vec{v}_{tor} &= (-l_0\vec{\omega}_0\sin(\beta_{tot}+q_f)-l_1\vec{\omega}_1\sin(\theta_1-\lambda)-\\ &l_2\vec{\omega}_2\sin(\pi-\theta_2+\lambda)+l_{tor}\vec{\omega}_{tor}\sin(\pi/2-\theta_{tor}-\lambda))I\\ &+(\vec{\omega}_1 l_1\cos(\theta_1-\lambda)+l_0\vec{\omega}_0\cos(\beta_{tot}+q_f)\\ &-l_2\vec{\omega}_2\cos(\pi-\theta_2+\lambda)-l_{tor}\vec{\omega}_{tor}\cos(\pi/2-\theta_{tor}-\lambda))K\end{aligned} \tag{29}$$

Accordingly, the linear acceleration of the links can be calculated easily. After generation of the robot trajectory paths with the aid of interpolation process and with utilization of MATLAB commands, the simulation of the biped robot can be performed. Based on the all above expressed relations and the resulted parameters and subsequently with inserting the parameters into the program, the simulation of the robot are presented in simulation results.

## 3. Dynamic of the robot

In similarity of human and the biped robots, the most important parameter of stability of the robot refers to ZMP. The ZMP (Zero moment point) is a point on the ground whose sum of all moments around this point is equal to zero. Totally, the ZMP mathematical formulation can be presented as below:

$$x_{zmp}=\frac{\sum_{i=1}^{n}m_i(g\cos\lambda+\ddot{z}_i)x_i-\sum_{i=1}^{n}m_i(g\sin\lambda+\ddot{x}_i)z_i-\sum_{i=1}^{n}{}^{i}I_i\ddot{\theta}_i}{\sum_{i=1}^{n}m_i(g\cos\lambda+\ddot{z}_i)} \tag{30}$$

Where, $\ddot{x}_i$ and $\ddot{z}_i$ are horizontal and vertical acceleration of the link's mass center with respect to F.C.S where $\ddot{\theta}_i$ is the angular acceleration of the links calculated from the interpolation process. On the other hand, the stability of the robot is determined according to attitude of ZMP. This means that if the ZMP be within the convex hull of the robot, the stable movement of the robot will be obtained and there are no interruptions in kinematic parameters (Velocity of the links). The convex hull can be imagined as a projection of a

pyramid with its heads on support and swing foots and also on the hip joint. Generally, the ZMP can be classified as the following cases:

1) **Moving ZMP**
2) **Fixed ZMP**

The moving type of the robot walking is similar to human gait. In the fixed type, the ZMP position is restricted through the support feet or the user's selected areas. Consequently, the significant torso's modified motion is required for stable walking of the robot. For the explained process, the program has been designed to find target angle of the torso for providing the fixed ZMP position automatically. In the designed program, $q_{torso}$ shows the deflection angle of the torso determined by the user or calculated by auto detector mood of the program. Note, in the mood of auto detector, the torso needed motion for obtaining the mentioned fixed ZMP will be extracted with respect to the desired ranges. The desired ranges include the defined support feet area by the users or automatically by the designed program. Note, the most affecting parameters for obtaining the robot's stable walking are the hip's height and position. By varying the parameters with iterative method for $x_{ed}, x_{sd}$ [Huang and et. Al, 2001] and choosing the optimum hip height, the robot control process with respect to the torso's modified angles and the mentioned parameters can be performed. To obtain the joint's actuator torques, the Lagrangian relation [Kraige, 1989] has been used at the single support phase as below:

$$\tau_i = H(q)\ddot{q} + C(q,\dot{q})\dot{q} + G(q_i) \tag{31}$$

where, $i = 0, 2, \cdots 6$ and $H, C, G$ are mass inertia, coriolis and gravitational matrices of the system which can be written as following:

$$H(q)=\begin{bmatrix} h_{11} & h_{12} & h_{13} & h_{14} & h_{15} & h_{16} & h_{17} \\ h_{21} & h_{22} & h_{23} & h_{24} & h_{25} & h_{26} & h_{27} \\ h_{31} & h_{32} & h_{33} & h_{34} & h_{35} & h_{36} & h_{37} \\ h_{41} & h_{42} & h_{43} & h_{44} & h_{45} & h_{46} & h_{47} \\ h_{51} & h_{52} & h_{53} & h_{54} & h_{55} & h_{56} & h_{57} \\ h_{61} & h_{62} & h_{63} & h_{64} & h_{65} & h_{66} & h_{67} \end{bmatrix} \quad C(q,\dot{q})=\begin{bmatrix} c_{11} & c_{12} & c_{13} & c_{14} & c_{15} & c_{16} & c_{17} \\ c_{21} & c_{22} & c_{23} & c_{24} & c_{25} & c_{26} & c_{27} \\ c_{31} & c_{32} & c_{33} & c_{34} & c_{35} & c_{36} & c_{37} \\ c_{41} & c_{42} & c_{43} & c_{44} & c_{45} & c_{46} & c_{47} \\ c_{51} & c_{52} & c_{53} & c_{54} & c_{55} & c_{56} & c_{57} \\ c_{61} & c_{62} & c_{63} & c_{64} & c_{65} & c_{66} & c_{67} \end{bmatrix} \quad G(q) = \begin{bmatrix} G_1 \\ G_2 \\ G_3 \\ G_4 \\ G_5 \\ G_{tor} \end{bmatrix}$$

Obviously, the above expressed matrices show the double support phase of the movement of the robot where they are used for the single support phase of the movement. On the other hand, the relation (31) is used for the single support phase of the robot. Within the double support phase of the robot, due to the occurrence impact between the swing leg and the ground, the modified shape of relation (31) is used with respect to effects of the reaction forces of the ground [Lum and et. Al. 1999 and Westervelt, 2003, and Hon and et. Al., 1978]. For the explained process and in order to obtain the single support phase equations of the robot, the value of $q_0$ (as can be seen in figure (1.4)) must be put equal to zero. The calculation process of the above mentioned matrices components contain bulk mathematical relations. Here, for avoiding the aforesaid relations, just the simplified relations are presented:

$$h_{11} = [m_1(l_{c1}^2 + l_{c1} l_e \cos(q_1 - \varphi))] + [m_2(l_1^2 + l_{c2}^2 + l_1 l_e \cos(q_1 - \varphi) + l_{c2} l_e \cos(q_2 - \varphi) + \cdots$$
$$2 l_1 l_{c2} \cos(q_2 - q_1))] + [m_3(l_1^2 + l_2^2 + l_{c3}^2 + l_1 l_e \cos(q_1 - \varphi) + l_2 l_e \cos(q_2 - \varphi) - l_{c3} l_e \cos(-q_3 + \varphi) + \cdots$$
$$2 l_1 l_2 \cos(q_2 - q_1) - 2 l_1 l_{c3} \cos(q_1 - q_3) - 2 l_2 l_{c3} \cos(q_2 - q_3))] + [m_4(l_1^2 + l_2^2 + l_3^2 + l_{c4}^2 + \cdots$$
$$l_1 l_e \cos(q_1 - \varphi) + l_2 l_e \cos(q_2 - \varphi) - l_3 l_e \cos(q_3 - \varphi) - l_{c4} l_e \cos(-q_4 + \varphi) + 2 l_1 l_2 \cos(q_2 - q_1) - \cdots$$
$$2 l_1 l_3 \cos(q_3 - q_1) - 2 l_1 l_{c4} \cos(q_1 - q_4) - 2 l_2 l_3 \cos(q_3 - q_2) - 2 l_2 l_{c4} \cos(q_2 - q_4) + 2 l_{c4} l_3 \cos(q_3 - q_4))] +$$
$$[m_5(l_1^2 + l_2^2 + l_3^2 + l_4^2 + l_{cfswing}^2 + l_1 l_e \cos(q_1 - \varphi) + l_2 l_e \cos(q_2 - \varphi) - l_3 l_e \cos(q_3 - \varphi) - \cdots$$
$$l_4 l_e \cos(q_4 - \varphi) - l_{cfswing} l_e \cos(\varphi - (\pi/2) + q_{fswing} - \beta_{fswing}) + 2 l_1 l_2 \cos(q_2 - q_1) - 2 l_1 l_3 \cos(q_3 - q_1) - \cdots$$
$$2 l_1 l_4 \cos(q_4 - q_1) - 2 l_1 l_{cfswing} \cos(q_1 - (\pi/2) + q_{fswing} - \beta_{fswing}) - 2 l_2 l_3 \cos(q_3 - q_2) - \cdots$$
$$2 l_2 l_4 \cos(q_4 - q_2) - 2 l_2 l_{cfswing} \cos(q_2 - (\pi/2) + q_{fswing} - \beta_{fswing}) + 2 l_3 l_4 \cos(q_4 - q_3) + \cdots$$
$$2 l_4 l_{cfswing} \cos(q_4 - (\pi/2) + q_{fswing} - \beta_{fswing}) + 2 l_3 l_{cfswing} \cos(q_3 - (\pi/2) + q_{fswing} - \beta_{fswing}))] + \cdots$$
$$[m_{tor}(l_1^2 + l_2^2 + l_{ctorso}^2 + l_1 l_e \cos(q_1 - \varphi) + l_2 l_e \cos(q_2 - \varphi) + l_e l_{ctorso} \cos(-q_{torso} - \varphi - (\pi/2)) + \cdots$$
$$2 l_1 l_2 \cos(q_2 - q_1) + 2 l_1 l_{ctorso} \cos(-q_{torso} - q_1 - (\pi/2)) + 2 l_2 l_{ctorso} \cos(q_{torso} + q_2 + (\pi/2))] + I_1 + I_2 + \cdots$$
$$I_3 + I_4 + I_5 + I_{torso}$$

$$h_{12} = [m_1(l_{c1}^2)] + [m_2(l_1^2 + l_{c2}^2 + 2 l_1 l_{c2} \cos(q_2 - q_1))] + [m_3(l_1^2 + l_2^2 + l_{c3}^2 + 2 l_1 l_2 \cos(q_2 - q_1) - \cdots$$
$$2 l_1 l_{c3} \cos(q_1 - q_3) - 2 l_2 l_{c3} \cos(q_2 - q_3))] + [m_4(l_1^2 + l_2^2 + l_3^2 + l_{c4}^2 + 2 l_1 l_2 \cos(q_2 - q_1) - \cdots$$
$$2 l_1 l_3 \cos(q_3 - q_1) - 2 l_1 l_{c4} \cos(q_1 - q_4) - 2 l_2 l_3 \cos(q_3 - q_2) - 2 l_2 l_{c4} \cos(q_2 - q_4) + 2 l_{c4} l_3 \cos(q_3 - q_4))] +$$
$$[m_5(l_1^2 + l_2^2 + l_3^2 + l_4^2 + l_{cfswing}^2 + 2 l_1 l_2 \cos(q_2 - q_1) - 2 l_1 l_3 \cos(q_3 - q_1) - 2 l_1 l_4 \cos(q_4 - q_1) - \cdots$$
$$2 l_1 l_{cfswing} \cos(q_1 - (\pi/2) + q_{fswing} - \beta_{fswing}) - 2 l_2 l_3 \cos(q_3 - q_2) - 2 l_2 l_4 \cos(q_4 - q_2) - \cdots$$
$$2 l_2 l_{cfswing} \cos(q_2 - (\pi/2) + q_{fswing} - \beta_{fswing}) + 2 l_3 l_4 \cos(q_4 - q_3) + \cdots$$
$$2 l_4 l_{cfswing} \cos(q_4 - (\pi/2) + q_{fswing} - \beta_{fswing}) + 2 l_3 l_{cfswing} \cos(q_3 - (\pi/2) + q_{fswing} - \beta_{fswing}))] + \cdots$$
$$[m_{tor}(l_1^2 + l_2^2 + l_{ctorso}^2 + 2 l_1 l_2 \cos(q_2 - q_1) + 2 l_1 l_{ctorso} \cos(-q_{torso} - q_1 - (\pi/2)) + \cdots$$
$$2 l_2 l_{ctorso} \cos(q_{torso} + q_2 + (\pi/2))] + I_1 + I_2 + I_3 + I_4 + I_5 + I_{torso}$$

$$h_{13} = [m_2(l_{c2}^2 + l_1 l_{c2}\cos(q_2 - q_1))] + [m_3(l_2^2 + l_{c3}^2 + l_1 l_2\cos(q_2 - q_1) - l_1 l_{c3}\cos(q_1 - q_3) - \cdots$$
$$2l_2 l_{c3}\cos(q_2 - q_3))] + [m_4(l_2^2 + l_3^2 + l_{c4}^2 + l_1 l_2\cos(q_2 - q_1) - l_1 l_3\cos(q_3 - q_1) - \cdots$$
$$l_1 l_{c4}\cos(q_1 - q_4) - 2l_2 l_3\cos(q_3 - q_2) - 2l_2 l_{c4}\cos(q_2 - q_4) + 2l_{c4} l_3\cos(q_3 - q_4))] + \cdots$$
$$[m_5(l_2^2 + l_3^2 + l_4^2 + l_{cfswing}^2 + l_1 l_2\cos(q_2 - q_1) - l_1 l_3\cos(q_3 - q_1) - l_1 l_4\cos(q_4 - q_1) - \cdots$$
$$l_1 l_{cfswing}\cos(q_1 - (\pi/2) + q_{fswing} - \beta_{fswing}) - 2l_2 l_3\cos(q_3 - q_2) - 2l_2 l_4\cos(q_4 - q_2) - \cdots$$
$$2l_2 l_{cfswing}\cos(q_2 - (\pi/2) + q_{fswing} - \beta_{fswing}) + 2l_3 l_4\cos(q_4 - q_3) + \cdots$$
$$2l_4 l_{cfswing}\cos(q_4 - (\pi/2) + q_{fswing} - \beta_{fswing}) + 2l_3 l_{cfswing}\cos(q_3 - (\pi/2) + q_{fswing} - \beta_{fswing}))] + \cdots$$
$$[m_{tor}(l_2^2 + l_{ctorso}^2 + l_1 l_2\cos(q_2 - q_1) + l_1 l_{ctorso}\cos(-q_{torso} - q_1 - (\pi/2)) + 2l_2 l_{ctorso}\cos(q_{torso} + q_2 + (\pi/2))]$$
$$+ I_2 + I_3 + I_4 + I_5 + I_{torso}$$

$$h_{14} = [m_3(l_{c3}^2 - l_1 l_{c3}\cos(q_1 - q_3) - l_2 l_{c3}\cos(q_2 - q_3))] + [m_4(l_3^2 + l_{c4}^2 - l_1 l_3\cos(q_3 - q_1) - \cdots$$
$$l_1 l_{c4}\cos(q_1 - q_4) - l_2 l_3\cos(q_3 - q_2) - l_2 l_{c4}\cos(q_2 - q_4) + 2l_{c4} l_3\cos(q_3 - q_4))] + [m_5(l_3^2 + l_4^2 + \cdots$$
$$l_{cfswing}^2 - l_1 l_3\cos(q_3 - q_1) - l_1 l_4\cos(q_4 - q_1) - l_1 l_{cfswing}\cos(q_1 - (\pi/2) + q_{fswing} - \beta_{fswing}) - \cdots$$
$$l_2 l_3\cos(q_3 - q_2) - l_2 l_4\cos(q_4 - q_2) - l_2 l_{cfswing}\cos(q_2 - (\pi/2) + q_{fswing} - \beta_{fswing}) + 2l_3 l_4\cos(q_4 - q_3) + \cdots$$
$$2l_4 l_{cfswing}\cos(q_4 - (\pi/2) + q_{fswing} - \beta_{fswing}) + 2l_3 l_{cfswing}\cos(q_3 - (\pi/2) + q_{fswing} - \beta_{fswing}))] + I_3 + I_4 + I_5$$

$$h_{15} = [m_4(l_{c4}^2 - l_1 l_{c4}\cos(q_1 - q_4) - l_2 l_{c4}\cos(q_2 - q_4) + l_{c4} l_3\cos(q_3 - q_4))] + [m_5(l_4^2 + \cdots$$
$$l_{cfswing}^2 - l_1 l_4\cos(q_4 - q_1) - l_1 l_{cfswing}\cos(q_1 - (\pi/2) + q_{fswing} - \beta_{fswing}) - l_2 l_4\cos(q_4 - q_2) - \cdots$$
$$l_2 l_{cfswing}\cos(q_2 - (\pi/2) + q_{fswing} - \beta_{fswing}) + l_3 l_4\cos(q_4 - q_3) + \cdots$$
$$2l_4 l_{cfswing}\cos(q_4 - (\pi/2) + q_{fswing} - \beta_{fswing}) + l_3 l_{cfswing}\cos(q_3 - (\pi/2) + q_{fswing} - \beta_{fswing}))] + I_4 + I_5$$

$$h_{16} = [m_5(l_{cfswing}^2 - l_1 l_{cfswing}\cos(q_1 - (\pi/2) + q_{fswing} - \beta_{fswing}) - l_2 l_{cfswing}\cos(q_2 - (\pi/2) + q_{fswing} - \beta_{fswing})$$
$$+ l_4 l_{cfswing}\cos(q_4 - (\pi/2) + q_{fswing} - \beta_{fswing}) + l_3 l_{cfswing}\cos(q_3 - (\pi/2) + q_{fswing} - \beta_{fswing}))] + I_5$$

$$h_{17} = [m_{torso}(l_{ctorso}^2 + l_1 l_{ctorso}\cos(-q_{torso} - (\pi/2) - q_1) + l_2 l_{ctorso}\cos(q_{torso} + (\pi/2) + q_2))] + I_{toroso}$$

$$h_{21} = [m_2(l_{c2}^2 + l_{c2}l_e\cos(q_2-\varphi) + l_1 l_{c2}\cos(q_2-q_1))] + [m_3(l_2^2 + l_{c3}^2 + l_2 l_e\cos(q_2-\varphi) - \cdots$$
$$l_{c3}l_e\cos(-q_3+\varphi) + l_1 l_2\cos(q_2-q_1) - l_1 l_{c3}\cos(q_1-q_3) - 2l_2 l_{c3}\cos(q_2-q_3))] + [m_4(l_2^2 + l_3^2 + l_{c4}^2 + \cdots$$
$$l_2 l_e\cos(q_2-\varphi) - l_3 l_e\cos(q_3-\varphi) - l_{c4}l_e\cos(-q_4+\varphi) + l_1 l_2\cos(q_2-q_1) - l_1 l_3\cos(q_3-q_1) - \cdots$$
$$l_1 l_{c4}\cos(q_1-q_4) - 2l_2 l_3\cos(q_3-q_2) - 2l_2 l_{c4}\cos(q_2-q_4) + 2l_{c4}l_3\cos(q_3-q_4))] + \cdots$$
$$[m_5(l_2^2 + l_3^2 + l_4^2 + l_{cfswing}^2 + l_2 l_e\cos(q_2-\varphi) - l_3 l_e\cos(q_3-\varphi) - l_4 l_e\cos(q_4-\varphi) - \cdots$$
$$l_{cfswing}l_e\cos(\varphi-(\pi/2)+q_{fswing}-\beta_{fswing}) + l_1 l_2\cos(q_2-q_1) - l_1 l_3\cos(q_3-q_1) - \cdots$$
$$l_1 l_4\cos(q_4-q_1) - l_1 l_{cfswing}\cos(q_1-(\pi/2)+q_{fswing}-\beta_{fswing}) - 2l_2 l_3\cos(q_3-q_2) - \cdots$$
$$2l_2 l_4\cos(q_4-q_2) - 2l_2 l_{cfswing}\cos(q_2-(\pi/2)+q_{fswing}-\beta_{fswing}) + 2l_3 l_4\cos(q_4-q_3) + \cdots$$
$$2l_4 l_{cfswing}\cos(q_4-(\pi/2)+q_{fswing}-\beta_{fswing}) + 2l_3 l_{cfswing}\cos(q_3-(\pi/2)+q_{fswing}-\beta_{fswing}))] + \cdots$$
$$[m_{tor}(l_2^2 + l_{ctorso}^2 + l_2 l_e\cos(q_2-\varphi) + l_e l_{ctorso}\cos(-q_{torso}-\varphi-(\pi/2)) + l_1 l_2\cos(q_2-q_1) + \cdots$$
$$l_1 l_{ctorso}\cos(-q_{torso}-q_1-(\pi/2)) + 2l_2 l_{ctorso}\cos(q_{torso}+q_2+(\pi/2))] + I_2 + I_3 + I_4 + I_5 + I_{torso}$$

$$h_{22} = [m_2(l_{c2}^2 + l_1 l_{c2}\cos(q_2-q_1))] + [m_3(l_2^2 + l_{c3}^2 + l_1 l_2\cos(q_2-q_1) - l_1 l_{c3}\cos(q_1-q_3) - \cdots$$
$$2l_2 l_{c3}\cos(q_2-q_3))] + [m_4(l_2^2 + l_3^2 + l_{c4}^2 + l_1 l_2\cos(q_2-q_1) - l_1 l_3\cos(q_3-q_1) - l_1 l_{c4}\cos(q_1-q_4) - \cdots$$
$$2l_2 l_3\cos(q_3-q_2) - 2l_2 l_{c4}\cos(q_2-q_4) + 2l_{c4}l_3\cos(q_3-q_4))] + [m_5(l_2^2 + l_3^2 + l_4^2 + l_{cfswing}^2 + \cdots$$
$$l_1 l_2\cos(q_2-q_1) - l_1 l_3\cos(q_3-q_1) - l_1 l_4\cos(q_4-q_1) - l_1 l_{cfswing}\cos(q_1-(\pi/2)+q_{fswing}-\beta_{fswing}) - 2l_2 l_3\cos(q_3-q_2) \cdots$$
$$-2l_2 l_4\cos(q_4-q_2) - 2l_2 l_{cfswing}\cos(q_2-(\pi/2)+q_{fswing}-\beta_{fswing}) + 2l_3 l_4\cos(q_4-q_3) + \cdots$$
$$2l_4 l_{cfswing}\cos(q_4-(\pi/2)+q_{fswing}-\beta_{fswing}) + 2l_3 l_{cfswing}\cos(q_3-(\pi/2)+q_{fswing}-\beta_{fswing}))] + \cdots$$
$$[m_{tor}(l_2^2 + l_{ctorso}^2 + l_1 l_2\cos(q_2-q_1) + l_1 l_{ctorso}\cos(-q_{torso}-q_1-(\pi/2)) + 2l_2 l_{ctorso}\cos(q_{torso}+q_2+(\pi/2))] + \cdots$$
$$I_2 + I_3 + I_4 + I_5 + I_{torso}$$

$$h_{23} = [m_2(l_{c2}^2)] + [m_3(l_2^2 + l_{c3}^2 - 2l_2 l_{c3}\cos(q_2-q_3))] + [m_4(l_2^2 + l_3^2 + l_{c4}^2 - 2l_2 l_3\cos(q_3-q_2) - \cdots$$
$$2l_2 l_{c4}\cos(q_2-q_4) + 2l_{c4}l_3\cos(q_3-q_4))] + [m_5(l_2^2 + l_3^2 + l_4^2 + l_{cfswing}^2 - 2l_2 l_3\cos(q_3-q_2) - 2l_2 l_4\cos(q_4-q_2) - \cdots$$
$$2l_2 l_{cfswing}\cos(q_2-(\pi/2)+q_{fswing}-\beta_{fswing}) + 2l_3 l_4\cos(q_4-q_3) + 2l_4 l_{cfswing}\cos(q_4-(\pi/2)+q_{fswing}-\beta_{fswing}) + \cdots$$
$$2l_3 l_{cfswing}\cos(q_3-(\pi/2)+q_{fswing}-\beta_{fswing}))] + [m_{tor}(l_2^2 + l_{ctorso}^2 + 2l_2 l_{ctorso}\cos(q_{torso}+q_2+(\pi/2))] + \cdots$$
$$I_2 + I_3 + I_4 + I_5 + I_{torso}$$

$$h_{24}=[m_3(l_{c3}^2-l_2l_{c3}\cos(q_2-q_3))]+[m_4(l_3^2+l_{c4}^2-l_2l_3\cos(q_3-q_2)-l_2l_{c4}\cos(q_2-q_4)+2l_{c4}l_3\cos(q_3-q_4))]+\cdots$$
$$[m_5(l_3^2+l_4^2+l_{cfswing}^2-l_2l_3\cos(q_3-q_2)-l_2l_4\cos(q_4-q_2)-l_2l_{cfswing}\cos(q_2-(\pi/2)+q_{fswing}-\beta_{fswing})+\cdots$$
$$2l_3l_4\cos(q_4-q_3)+2l_4l_{cfswing}\cos(q_4-(\pi/2)+q_{fswing}-\beta_{fswing})+2l_3l_{cfswing}\cos(q_3-(\pi/2)+q_{fswing}-\beta_{fswing}))]+\cdots$$
$$I_3+I_4+I_5$$

$$h_{25}=[m_4(l_{c4}^2-l_2l_{c4}\cos(q_2-q_4)+l_{c4}l_3\cos(q_3-q_4))]+[m_5(l_4^2+l_{cfswing}^2-l_2l_4\cos(q_4-q_2)-\cdots$$
$$l_2l_{cfswing}\cos(q_2-(\pi/2)+q_{fswing}-\beta_{fswing})+l_3l_4\cos(q_4-q_3)+2l_4l_{cfswing}\cos(q_4-(\pi/2)+q_{fswing}-\beta_{fswing})+\cdots$$
$$l_3l_{cfswing}\cos(q_3-(\pi/2)+q_{fswing}-\beta_{fswing}))]+I_4+I_5$$

$$h_{26}=[m_5(l_{cfswing}^2-l_2l_{cfswing}\cos(q_2-(\pi/2)+q_{fswing}-\beta_{fswing})+l_4l_{cfswing}\cos(q_4-(\pi/2)+q_{fswing}-\beta_{fswing})+\cdots$$
$$l_3l_{cfswing}\cos(q_3-(\pi/2)+q_{fswing}-\beta_{fswing}))]+I_5$$

$$h_{27}=[m_{torso}(l_{ctorso}^2+l_2l_{ctorso}\cos(q_{torso}+(\pi/2)+q_2)]+I_{torso}$$

$$h_{31}=[m_3(l_{c3}^2-l_{c3}l_e\cos(-q_3+\varphi)-l_1l_{c3}\cos(q_1-q_3)-l_2l_{c3}\cos(q_2-q_3))]+[m_4(l_3^2+l_{c4}^2-\cdots$$
$$l_3l_e\cos(q_3-\varphi)-l_{c4}l_e\cos(-q_4+\varphi)-l_1l_3\cos(q_3-q_1)-l_1l_{c4}\cos(q_1-q_4)-l_2l_3\cos(q_3-q_2)-\cdots$$
$$l_2l_{c4}\cos(q_2-q_4)+2l_{c4}l_3\cos(q_3-q_4))]+[m_5(l_3^2+l_4^2+l_{cfswing}^2-l_3l_e\cos(q_3-\varphi)-\cdots$$
$$l_4l_e\cos(q_4-\varphi)-l_{cfswing}l_e\cos(\varphi-(\pi/2)+q_{fswing}-\beta_{fswing})-l_1l_3\cos(q_3-q_1)-\cdots$$
$$l_1l_4\cos(q_4-q_1)-l_1l_{cfswing}\cos(q_1-(\pi/2)+q_{fswing}-\beta_{fswing})-l_2l_3\cos(q_3-q_2)-\cdots$$
$$l_2l_4\cos(q_4-q_2)-l_2l_{cfswing}\cos(q_2-(\pi/2)+q_{fswing}-\beta_{fswing})+2l_3l_4\cos(q_4-q_3)+\cdots$$
$$2l_4l_{cfswing}\cos(q_4-(\pi/2)+q_{fswing}-\beta_{fswing})+2l_3l_{cfswing}\cos(q_3-(\pi/2)+q_{fswing}-\beta_{fswing}))]+I_3+I_4+I_5$$

$$h_{32} = [m_3(l_{c3}^2 - l_1 l_{c3}\cos(q_1 - q_3) - l_2 l_{c3}\cos(q_2 - q_3))] + [m_4(l_3^2 + l_{c4}^2 - l_1 l_3\cos(q_3 - q_1) - \cdots$$
$$l_1 l_{c4}\cos(q_1 - q_4) - l_2 l_3\cos(q_3 - q_2) - l_2 l_{c4}\cos(q_2 - q_4) + 2 l_{c4} l_3\cos(q_3 - q_4))] + [m_5(l_3^2 + l_4^2 + \cdots$$
$$l_{cfswing}^2 - l_1 l_3\cos(q_3 - q_1) - l_1 l_4\cos(q_4 - q_1) - l_1 l_{cfswing}\cos(q_1 - (\pi/2) + q_{fswing} - \beta_{fswing}) - \cdots$$
$$l_2 l_3\cos(q_3 - q_2) - l_2 l_4\cos(q_4 - q_2) - l_2 l_{cfswing}\cos(q_2 - (\pi/2) + q_{fswing} - \beta_{fswing}) + 2 l_3 l_4\cos(q_4 - q_3) + \cdots$$
$$2 l_4 l_{cfswing}\cos(q_4 - (\pi/2) + q_{fswing} - \beta_{fswing}) + 2 l_3 l_{cfswing}\cos(q_3 - (\pi/2) + q_{fswing} - \beta_{fswing}))] + \cdots$$
$$I_3 + I_4 + I_5$$

$$h_{33} = [m_3(l_{c3}^2 - l_2 l_{c3}\cos(q_2 - q_3))] + [m_4(l_3^2 + l_{c4}^2 - l_2 l_3\cos(q_3 - q_2) - l_2 l_{c4}\cos(q_2 - q_4) + 2 l_{c4} l_3\cos(q_3 - q_4))] + \cdots$$
$$[m_5(l_3^2 + l_4^2 + l_{cfswing}^2 - l_2 l_3\cos(q_3 - q_2) - l_2 l_4\cos(q_4 - q_2) - l_2 l_{cfswing}\cos(q_2 - (\pi/2) + q_{fswing} - \beta_{fswing}) + \cdots$$
$$2 l_3 l_4\cos(q_4 - q_3) + 2 l_4 l_{cfswing}\cos(q_4 - (\pi/2) + q_{fswing} - \beta_{fswing}) + 2 l_3 l_{cfswing}\cos(q_3 - (\pi/2) + q_{fswing} - \beta_{fswing}))] + \cdots$$
$$+ I_3 + I_4 + I_5$$

$$h_{34} = [m_3(l_{c3}^2)] + [m_4(l_3^2 + l_{c4}^2 + 2 l_{c4} l_3\cos(q_3 - q_4))] + [m_5(l_3^2 + l_4^2 + l_{cfswing}^2 + 2 l_3 l_4\cos(q_4 - q_3) + \cdots$$
$$2 l_4 l_{cfswing}\cos(q_4 - (\pi/2) + q_{fswing} - \beta_{fswing}) + 2 l_3 l_{cfswing}\cos(q_3 - (\pi/2) + q_{fswing} - \beta_{fswing}))] + \cdots$$
$$+ I_3 + I_4 + I_5$$

$$h_{35} = [m_4(l_{c4}^2 + l_{c4} l_3\cos(q_3 - q_4))] + [m_5(l_4^2 + l_{cfswing}^2 + l_3 l_4\cos(q_4 - q_3) + \cdots$$
$$2 l_4 l_{cfswing}\cos(q_4 - (\pi/2) + q_{fswing} - \beta_{fswing}) + l_3 l_{cfswing}\cos(q_3 - (\pi/2) + q_{fswing} - \beta_{fswing}))] + I_4 + I_5$$

$$h_{36} = [m_5(l_{cfswing}^2 + l_4 l_{cfswing}\cos(q_4 - (\pi/2) + q_{fswing} - \beta_{fswing}) + l_3 l_{cfswing}\cos(q_3 - (\pi/2) + q_{fswing} - \beta_{fswing}))] + I_5$$

$$h_{37} = 0$$

$$h_{41}=[m_4(l_{c4}^2-l_{c4}l_e\cos(-q_4+\varphi)-l_1l_{c4}\cos(q_1-q_4)-l_2l_{c4}\cos(q_2-q_4)+l_{c4}l_3\cos(q_3-q_4))]+\cdots$$
$$[m_5(l_4^2+l_{cfswing}^2-l_4l_e\cos(q_4-\varphi)-l_{cfswing}l_e\cos(\varphi-(\pi/2)+q_{fswing}-\beta_{fswing})-l_1l_4\cos(q_4-q_1)-\cdots$$
$$l_1l_{cfswing}\cos(q_1-(\pi/2)+q_{fswing}-\beta_{fswing})-l_2l_4\cos(q_4-q_2)-l_2l_{cfswing}\cos(q_2-(\pi/2)+q_{fswing}-\beta_{fswing})+\cdots$$
$$l_3l_4\cos(q_4-q_3)+2l_4l_{cfswing}\cos(q_4-(\pi/2)+q_{fswing}-\beta_{fswing})+l_3l_{cfswing}\cos(q_3-(\pi/2)+q_{fswing}-\beta_{fswing}))]+\cdots$$
$$I_4+I_5$$

$$h_{42}=[m_4(l_{c4}^2-l_1l_{c4}\cos(q_1-q_4)-l_2l_{c4}\cos(q_2-q_4)+l_{c4}l_3\cos(q_3-q_4))]+[m_5(l_4^2+l_{cfswing}^2-\cdots$$
$$l_1l_4\cos(q_4-q_1)-l_1l_{cfswing}\cos(q_1-(\pi/2)+q_{fswing}-\beta_{fswing})-l_2l_4\cos(q_4-q_2)-\cdots$$
$$l_2l_{cfswing}\cos(q_2-(\pi/2)+q_{fswing}-\beta_{fswing})+l_3l_4\cos(q_4-q_3)+2l_4l_{cfswing}\cos(q_4-(\pi/2)+q_{fswing}-\beta_{fswing})+\cdots$$
$$l_3l_{cfswing}\cos(q_3-(\pi/2)+q_{fswing}-\beta_{fswing}))]+I_4+I_5$$

$$h_{43}=[m_4(l_{c4}^2-l_2l_{c4}\cos(q_2-q_4)+l_{c4}l_3\cos(q_3-q_4))]+[m_5(l_4^2+l_{cfswing}^2-l_2l_4\cos(q_4-q_2)-\cdots$$
$$l_2l_{cfswing}\cos(q_2-(\pi/2)+q_{fswing}-\beta_{fswing})+l_3l_4\cos(q_4-q_3)+2l_4l_{cfswing}\cos(q_4-(\pi/2)+q_{fswing}-\beta_{fswing})+\cdots$$
$$l_3l_{cfswing}\cos(q_3-(\pi/2)+q_{fswing}-\beta_{fswing}))]+I_4+I_5$$

$$h_{44}=[m_4(l_{c4}^2+l_{c4}l_3\cos(q_3-q_4))]+[m_5(l_4^2+l_{cfswing}^2-l_2l_4\cos(q_4-q_2)+l_3l_4\cos(q_4-q_3)+\cdots$$
$$2l_4l_{cfswing}\cos(q_4-(\pi/2)+q_{fswing}-\beta_{fswing})+l_3l_{cfswing}\cos(q_3-(\pi/2)+q_{fswing}-\beta_{fswing}))]+I_4+I_5$$

$$h_{45}=[m_4(l_{c4}^2)]+[m_5(l_4^2+l_{cfswing}^2+2l_4l_{cfswing}\cos(q_4-(\pi/2)+q_{fswing}-\beta_{fswing}))]+I_4+I_5$$

$$h_{46}=[m_5(l_{cfswing}^2+l_4l_{cfswing}\cos(q_4-(\pi/2)+q_{fswing}-\beta_{fswing}))]+I_5$$

$$h_{47}=0$$

$$h_{51}=[m_5(l_{cfswing}^2-l_{cfswinge}l_e\cos(\varphi-(\pi/2)+q_{fswing}-\beta_{fswing})-l_1l_{cfswing}\cos(q_1-(\pi/2)+q_{fswing}-\beta_{fswing})-\cdots$$
$$l_2l_{cfswing}\cos(q_2-(\pi/2)+q_{fswing}-\beta_{fswing})+l_4l_{cfswing}\cos(q_4-(\pi/2)+q_{fswing}-\beta_{fswing})+\cdots$$
$$l_3l_{cfswing}\cos(q_3-(\pi/2)+q_{fswing}-\beta_{fswing}))]+I_5$$

$$h_{52}=[m_5(l_{cfswing}^2-l_1l_{cfswing}\cos(q_1-(\pi/2)+q_{fswing}-\beta_{fswing})-l_2l_{cfswing}\cos(q_2-(\pi/2)+q_{fswing}-\beta_{fswing})+\cdots$$
$$l_4l_{cfswing}\cos(q_4-(\pi/2)+q_{fswing}-\beta_{fswing})+l_3l_{cfswing}\cos(q_3-(\pi/2)+q_{fswing}-\beta_{fswing}))]+I_5$$

$$h_{53}=[m_5(l_{cfswing}^2-l_2l_{cfswing}\cos(q_2-(\pi/2)+q_{fswing}-\beta_{fswing})+\cdots$$
$$l_4l_{cfswing}\cos(q_4-(\pi/2)+q_{fswing}-\beta_{fswing})+l_3l_{cfswing}\cos(q_3-(\pi/2)+q_{fswing}-\beta_{fswing}))]+I_5$$

$$h_{54}=[m_5(l_{cfswing}^2+l_4l_{cfswing}\cos(q_4-(\pi/2)+q_{fswing}-\beta_{fswing})+l_3l_{cfswing}\cos(q_3-(\pi/2)+q_{fswing}-\beta_{fswing}))]+I_5$$

$$h_{55}=[m_5(l_{cfswing}^2+l_4l_{cfswing}\cos(q_4-(\pi/2)+q_{fswing}-\beta_{fswing}))]+I_5$$

$$h_{56}=[m_5(l_{cfswing}^2)]+I_5$$

$$h_{57}=0$$

$$h_{61}=[masstorso(l_{tor}^2+l_el_{tor}\cos(-q_{torso}-(\pi/2)-\varphi)+l_1l_{tor}\cos(-q_{torso}-(\pi/2)-q_1)+\cdots$$
$$l_2l_{tor}\cos(q_{torso}+(\pi/2)+q_2))]+I_{torso}$$

$$h_{62} = [masstorso(l_{tor}^2 + l_1 l_{tor}\cos(-q_{torso} - (\pi/2) - q_1) + l_2 l_{tor}\cos(q_{torso} + (\pi/2) + q_2))] + I_{torso}$$

$$h_{63} = [masstorso(l_{tor}^2 + l_2 l_{tor}\cos(q_{torso} + (\pi/2) + q_2))] + I_{torso}$$

$$h_{67} = [masstorso(l_{tor}^2)] + I_{torso}\,, h_{64,65,66} = 0$$

In the all of above mentioned components, the following parameters have been used and they can be seen in figure (1.6) :

$$\phi = \beta_{m.c} + q_0\,,\ \varphi = \lambda + q_0 + \beta_{m.c}\,,. \tag{32}$$

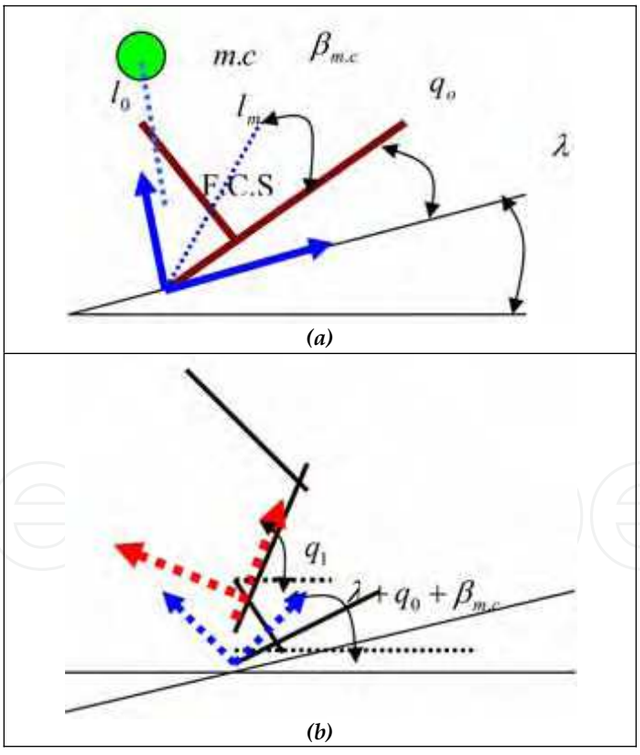


Fig. (1.6). (a) The foot's and (b) The support link's geometrical configurations.

Where, $l_{fswing}$ and $\beta_{fswing}$ refer to indexes of the swing leg with respect to geometrical configurations of the mass center of the swing leg as can be deducted from figure (1.6). The coriolis and gravitational components of the relation (30) can be calculated easily. After calculation of kinematic and dynamic parameters of the robot, the control process of the system will be emerged. In summery, the adaptive control procedure has been used for a known seven link biped robot. The more details and the related definitions such as the known and unknown system with respect to control aspect can be found in reference [Musavi and Bagheri, 2007 and Musavi, 2006, and Bagheri and Felezi, and et. Al., 2006]. For the simulation of the robot, the obtained parameters and relations are inserted into the designed program in Matlab environment. As can be seen in simulation results section, the most concerns refer to stability of the robot with respect to the important affecting parameters of the robot movements which indicate the ankle and hip joints parameters [Bagheri and Najafi and et. Al. 2006]. As can be seen from the simulations figures, the hip height and horizontal positions have considerable effects over the position of the ZMP and subsequently over the stability of the robot. To minimize the driver actuator torques of the joints, especially for the knee joint of the robot, the hip height which measured from the F.C.S has drastic role for diminution of the torques.

## 4. Simulation Results

In the designed program, the mentioned simulation processes for the two types of ZMP have been used for both of the nominal and un-nominal gait. For the un-nominal walking of the robot, the hip parameters (hip height) have been changed to consider the effects of the un-nominal motion upon the joint's actuator torques. The results are presented in figures (1.8) to (1.15) while the robot walks over declined surfaces for the single phase of the walking. Figure (1.15) shows combined path of the robot. The used specifications of the simulation of the robot are listed in table No. 1. Figures (1.8), (1.10) and (1.12) display the moving type of ZMP with the nominal walking of the robot. Figures (1.9), (1.11) and (1.13) show the same type of ZMP and also the un-nominal walking of the robot (with the changed hip height form the fixed coordinate system). Figure (1.14) shows the fixed ZMP upon descending surface. As can been seen from the table, the swing and support legs have the same geometrical and inertial values whereas in the designed program the users can choose different specifications. Note, the swing leg impact and the ground has been regarded in the designed program as given in references [Lum and et. Al. 1999 and Westervelt, 2003, and Hon and et. Al., 1978]. Below, the saggital movement and stability analysis of the seven link biped robot has been considered whereas the frontal considerations are neglected. For convenience, 3D simulations of the biped robot are presented. In table No. 1, $l_{an}, l_{ab}$ and $l_{af}$ present the foot profile which are displayed in figure (1.7). The program enables the user to compare the results as presented in figures where the paths for the single phase walking of the robot have been concerned. In the program with the aid of the given break points, either third-order spline or Vandermonde Matrix has been used for providing the different trajectory paths. With the aid of the designed program, the kinematic, dynamic and control parameters have been evaluated. Also,

the two types of ZMP have been investigated. The presented simulations indicate the hip height effects over joint's actuator torques for minimizing energy consumption and especially obtaining fine stability margin. As can be seen in figures (9.h), (11.h) and (13.h), for the un-nominal walking of the robot with the lower hip height, the knee's actuator torque values is more than the obtained values as shown in figures (8.h), (10.h) and (12.h) (for the nominal gait with the higher hip height). This is due to the robot's need to bend its knee joint more at a low hip position. Therefore, the large knee joint torque is required to support the robot. Therefore, for reducing the load on the knee joint and consequently with respect to minimum energy consumption, it is essential to keep the hip at a high position. Finally, the trajectory path generation needs more precision with respect to the obtained kinematic relations to avoid the link's velocity discontinuities. The presented results have an acceptable consistency with the typical robot.

| $l_{Sh.}$ | $l_{Ti..}$ | $l_{To.}$ | $l_{an}$ | $l_{ab}$ | $l_{af}$ |
|---|---|---|---|---|---|
| $0.3m$ | $0.3m$ | $0.3m$ | $0.1m$ | $0.1m$ | $0.13m$ |
| $m_{Sh.}$ | $m_{Th.}$ | $m_{To.}$ | $m_{Fo.}$ | $D_s$ | $T_c$ |
| $5.7kg$ | $10kg$ | $43kg$ | $3.3kg$ | $0.5m$ | $0.9s$ |
| $T_d$ | $T_m$ | $H_{ao}$ | $L_{ao}$ | $x_{ed}$ | $x_{sd}$ |
| $0.18s$ | $0.4s$ | $0.16m$ | $0.4m$ | $0.23m$ | $0.23m$ |
| $g_{gs}$ | $g_{gf}$ | $H_{\min}$ | $H_{\max}$ | $h_s$ | $H_s$ |
| 0 | 0 | $0.60m$ | $0.62m$ | $0.1m$ | $0.15m$ |
| $I_{shank}$ | | $I_{tight}$ | $I_{torso}$ | $I_{foot}$ | |
| $0.02kgm^2$ | | $0.08kgm^2$ | $1.4kgm^2$ | $0.01kgm^2$ | |

Table 1. The simulated robot specifications.

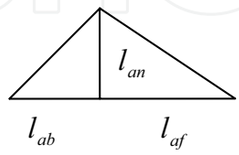


Fig. 1.7. The foot configuration.

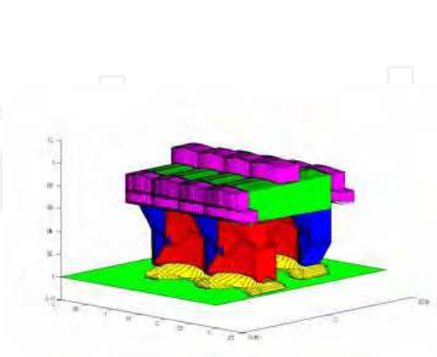

*(a) Stick Diagram*

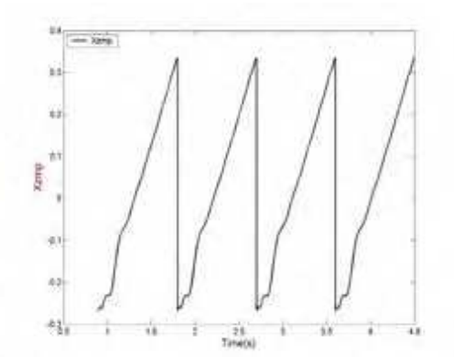

*(b) ZMP*

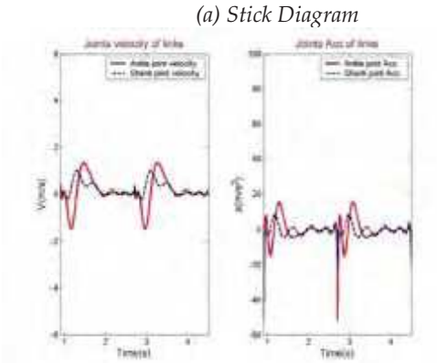

*(c) Velocity*



*(d) Acceleration*

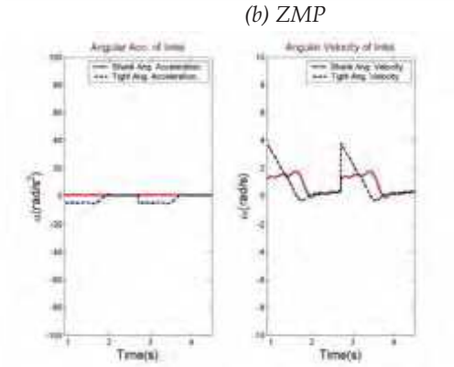

*(e) Angular Vel. (f) Angular Acc.*

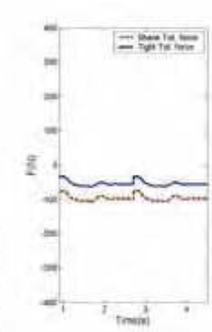

*(j) Inertial Forces*

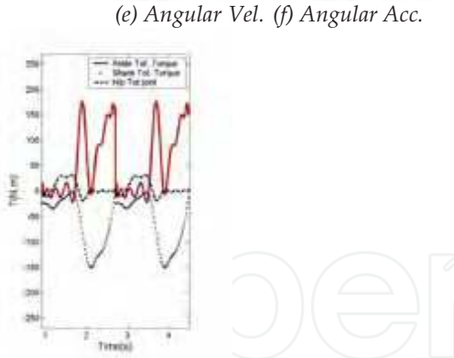

*(h) Driver Torques*

Fig. 1.8. *(a) The robot's stick diagram on* $\lambda = 0^{\circ}$ *, Moving ZMP,* $H_{\min}$ $0.60m, H_{\max}$ $0.62m$ *(b) The moving ZMP diagram in nominal gait which satisfies stability criteria (c) __: Shank M.C velocity, --: Tight M.C velocity (d)__: Shank M.C acceleration, --:Tight M.C acceleration (e) __: Shank angular velocity, --: Tight angular velocity (f) __: Shank angular acceleration, --: Tight angular acceleration (j) __: Shank M.C inertial force, --: Tight M.C inertial force (h) __: Ankle joint torque, --: Hip joint torque, …: Shank joint torque*

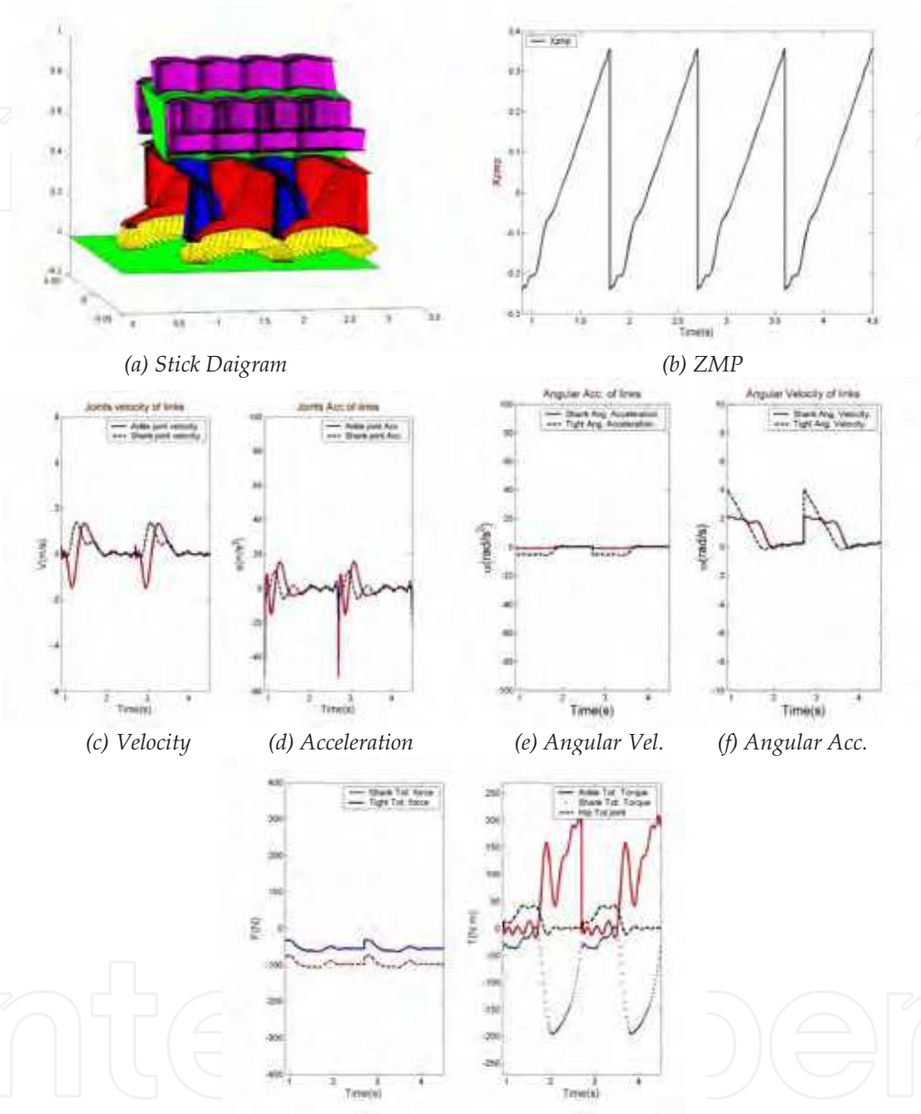

*(a) Stick Daigram* *(b) ZMP*

*(c) Velocity* *(d) Acceleration* *(e) Angular Vel.* *(f) Angular Acc.*

*(j) Inertial Forces* *(h) Driver Torques*

Fig. 1.9. *(a) The robot's stick diagram on* $\lambda \quad 0^{\circ}$ *, Moving ZMP,* $H_{\min} = 0.50m, H_{\max} = 0.52m$ *(b) The moving ZMP diagram in nominal gait which satisfies stability criteria (c) __: Shank M.C velocity, --: Tight M.C velocity (d)__: Shank M.C acceleration, --:Tight M.C acceleration (e) __: Shank angular velocity, --: Tight angular velocity (f) __: Shank angular acceleration, --: Tight angular acceleration (j) __: Shank M.C inertial force, --: Tight M.C inertial force (h) __: Ankle joint torque, --: Hip joint torque, …: Shank joint torque*

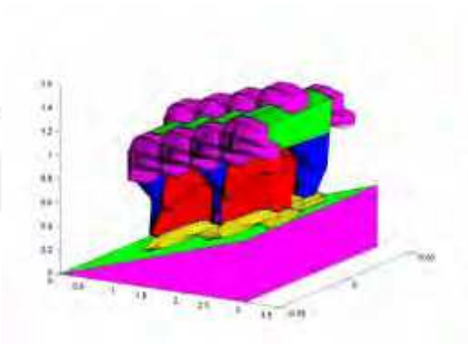

*(a) Stick Diagram*

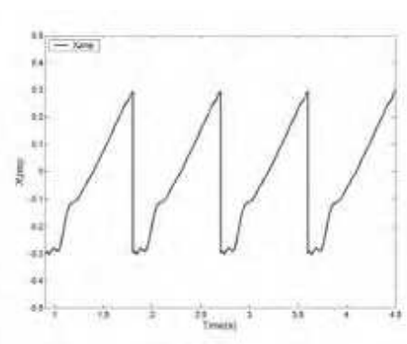

*(b) ZMP*

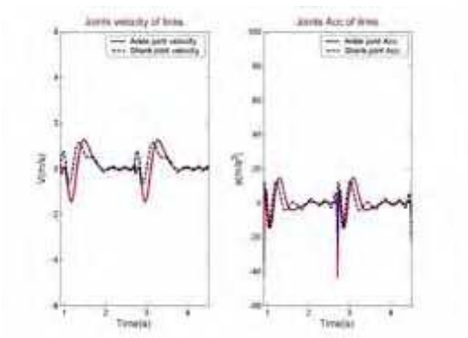

*(c) Velocity (d) Acceleration*

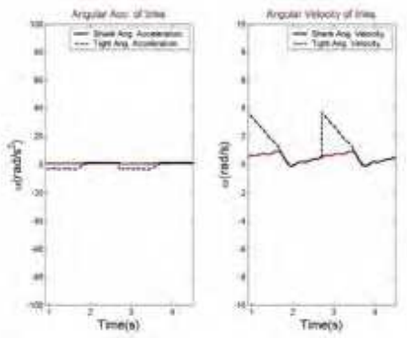

*(e) Angular Vel. (f) Angular Acc.*

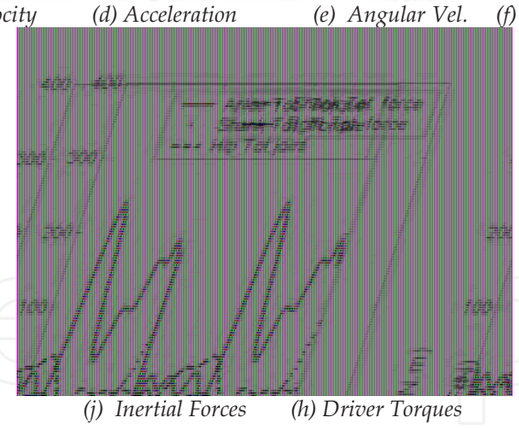

*(j) Inertial Forces (h) Driver Torques*

*Fig. 1.10 (a) The robot's stick diagram on $\lambda = 10^{\circ}$ , Moving ZMP, $H_{\min} = 0.60m, H_{\max} = 0.62m$ (b) The moving ZMP diagram in nominal gait which satisfies stability criteria (c) __: Shank M.C velocity, --: Tight M.C velocity (d)__: Shank M.C acceleration, --:Tight M.C acceleration (e) __: Shank angular velocity, --: Tight angular velocity (f) __: Shank angular acceleration, --: Tight angular acceleration (j) __: Shank M.C inertial force, --: Tight M.C inertial force (h) __: Ankle joint torque, --: Hip joint torque, …: Shank joint torque*

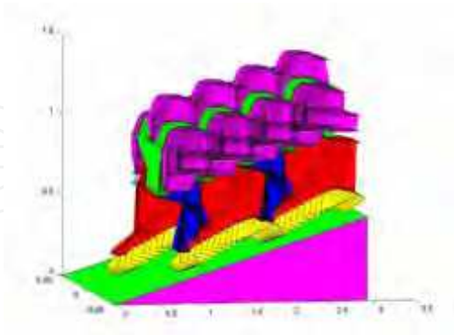

*(a) Stick Diagram*

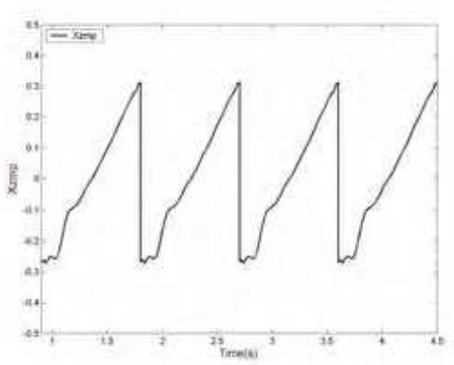


*(b) ZMP*

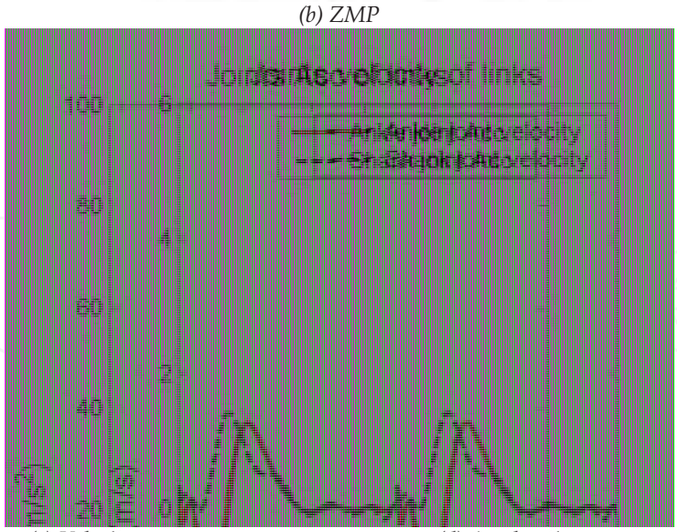


*(c) Velocity* *(d) Acceleration*

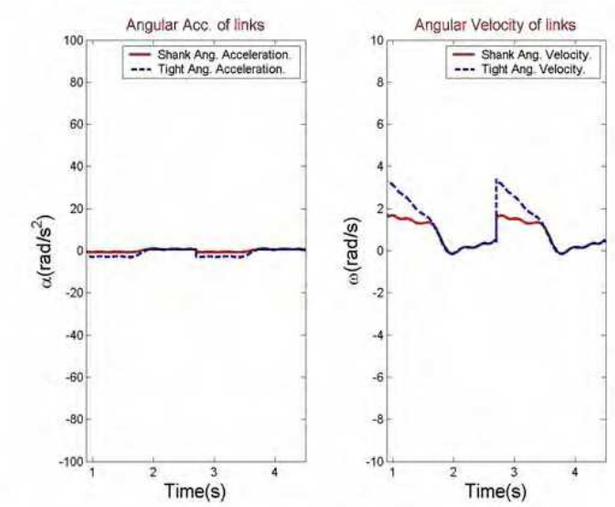


*(e) Angular Vel.* *(f) Angular Acc.*

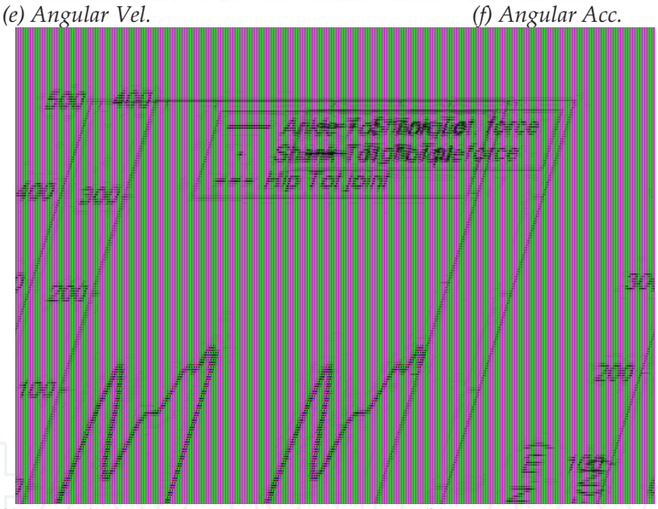


*(j) Inertial Forces* *(h) Driver Torques*

Fig. 1.11.

*(a) The robot's stick diagram on* $\lambda = 10^{\circ}$ *, Moving ZMP,* $H_{\min}$ $0.50m, H_{\max}$ $0.52m$

*(b) The moving ZMP diagram in nominal gait which satisfies stability criteria*

*(c) __: Shank M.C velocity, --: Tight M.C velocity*

*(d)__: Shank M.C acceleration, --:Tight M.C acceleration*

*(e) __: Shank angular velocity, --: Tight angular velocity*

*(f) __: Shank angular acceleration, --: Tight angular acceleration*

*(j) __: Shank M.C inertial force, --: Tight M.C inertial force*

*(h) __: Ankle joint torque, --: Hip joint torque, …: Shank joint torque*

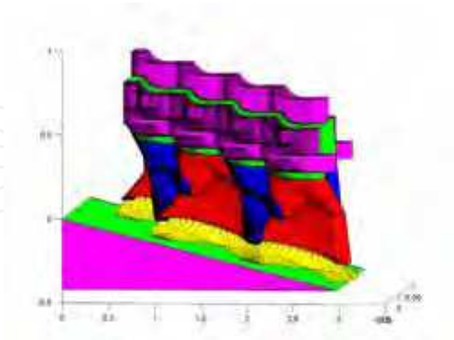

*(a) Stick Diagram*

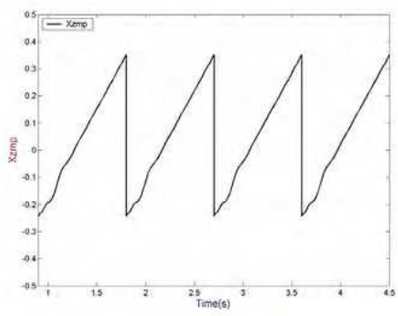


*(b) ZMP*

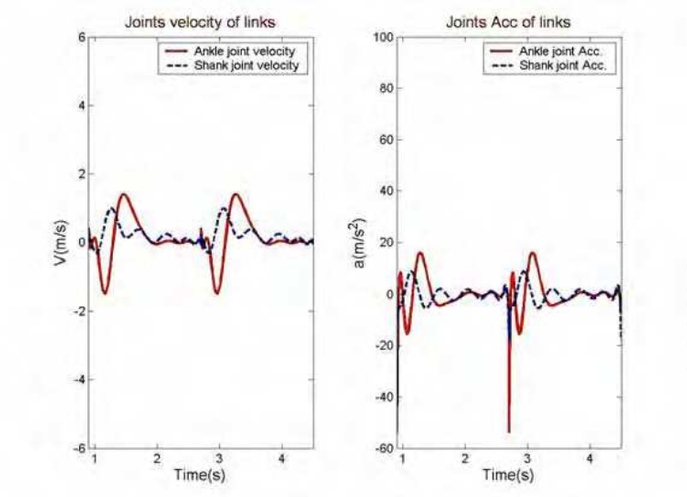


*(c) Velocity* *(d) Acceleration*

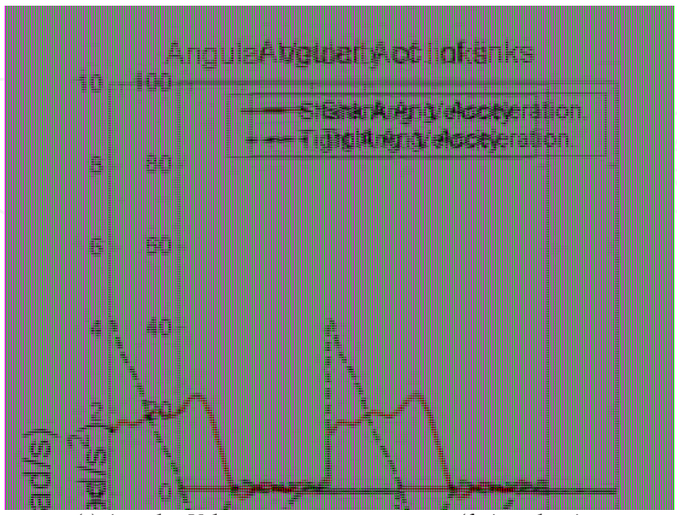


*(e) Angular Vel.* *(f) Angular Acc.*

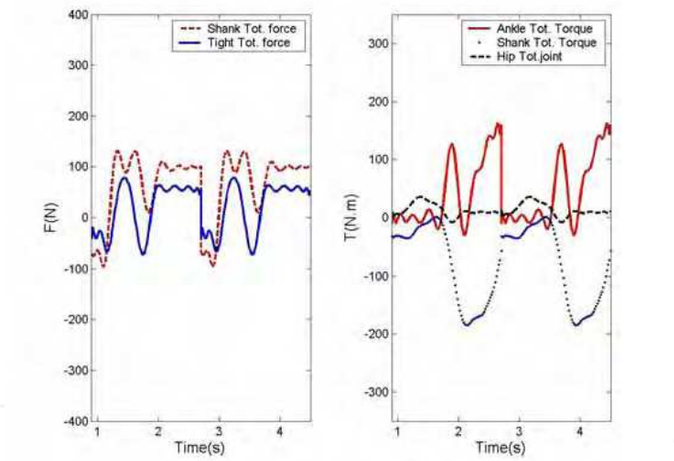


*(j) Inertial Forces* *(h) Driver Torques*

Fig. 1.12.

*(a) The robot's stick diagram on* $\lambda = -8^{\circ}$ *, Moving ZMP,* $H_{\min} = 0.60m, H_{\max} = 0.62m$

*(b) The moving ZMP diagram in nominal gait which satisfies stability criteria*

*(c) __: Shank M.C velocity, --: Tight M.C velocity*

*(d)__: Shank M.C acceleration, --:Tight M.C acceleration*

*(e) __: Shank angular velocity, --: Tight angular velocity*

*(f) __: Shank angular acceleration, --: Tight angular acceleration*

*(j) __: Shank M.C inertial force, --: Tight M.C inertial force*

*(h) __: Ankle joint torque, --: Hip joint torque, ….: Shank joint torque*

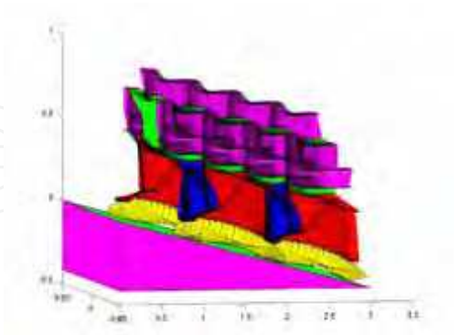

*(a) Stick Diagram*

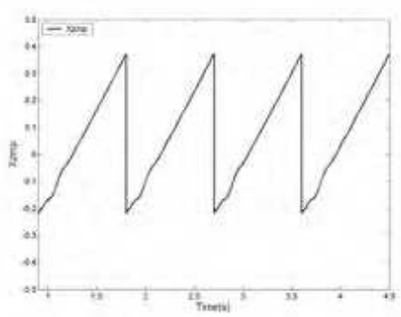

*(b) ZMP*

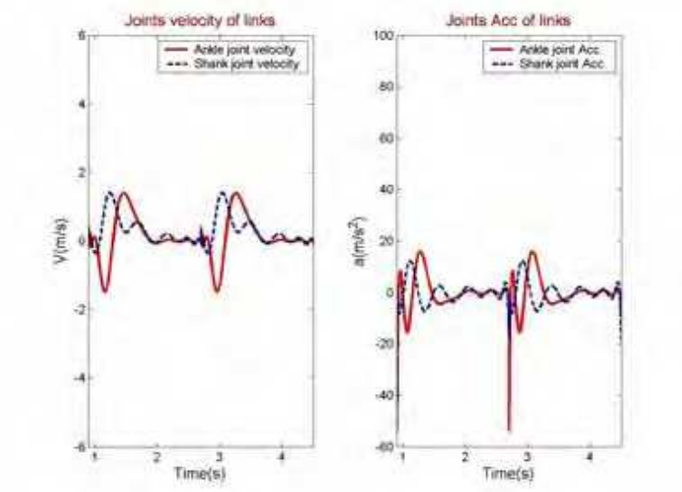


*(c) Velocity* *(d) Acceleration*

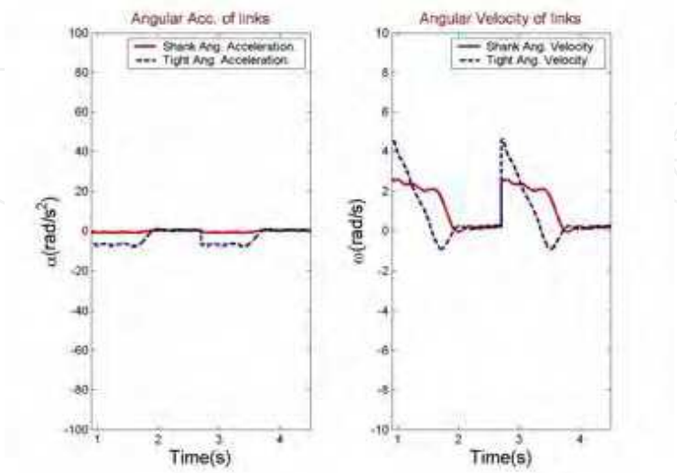


*(e) Angular Vel.* *(f) Angular Acc.*

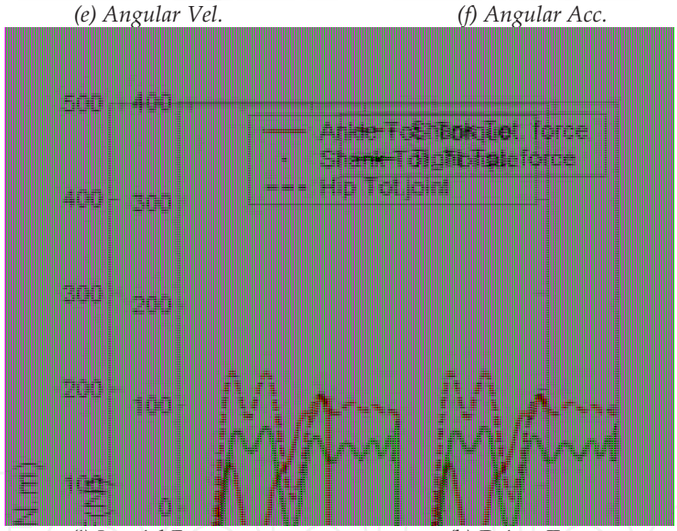


*(j) Inertial Forces* *(h) Driver Torques*

Fig. 1.13

*(a) The robot's stick diagram on* $\lambda = -8^{\circ}$ *, Moving ZMP,* $H_{\min} = 0.50m, H_{\max} = 0.52m$

*(b) The moving ZMP diagram in nominal gait which satisfies stability criteria*

*(c) __: Shank M.C velocity, --: Tight M.C velocity*

*(d)__: Shank M.C acceleration, --:Tight M.C acceleration*

*(e) __: Shank angular velocity, --: Tight angular velocity*

*(f) __: Shank angular acceleration, --: Tight angular acceleration*

*(j) __: Shank M.C inertial force, --: Tight M.C inertial force*

*(h) __: Ankle joint torque, --: Hip joint torque, ….: Shank joint torque*

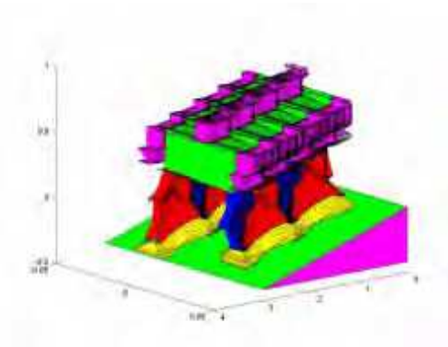

*(a) Stick Diagram*

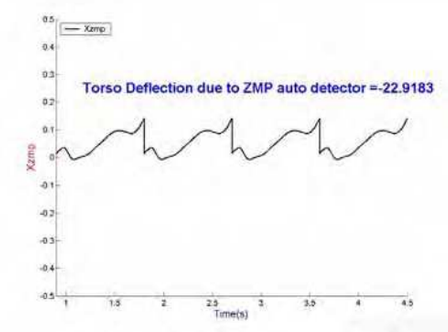


*(b) ZMP*

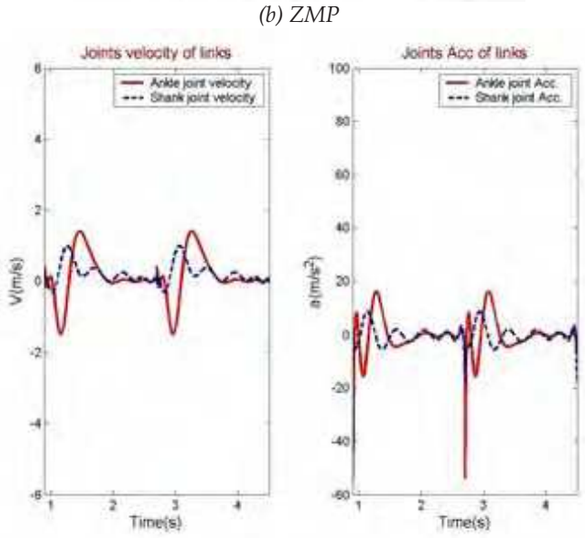


*(c) Velocity* *(d) Acceleration*

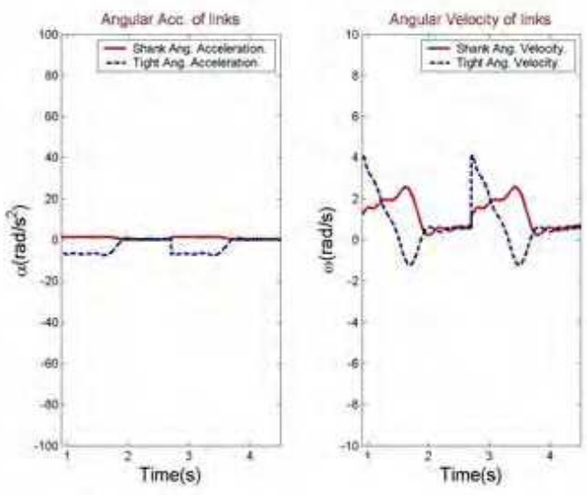


*e) Angular Vel.* *(f) Angular Acc.*

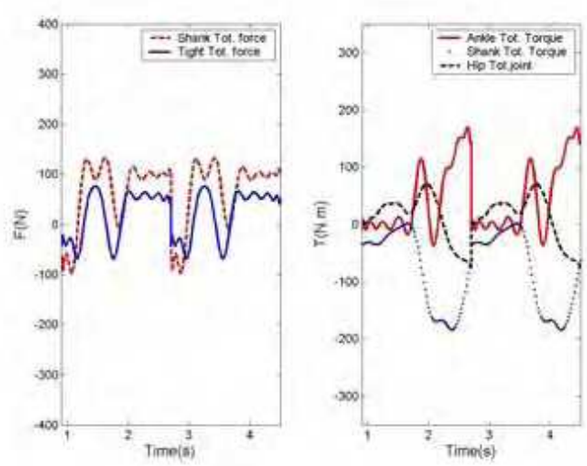


*(j) Inertial Forces* *(h) Driver Torques*

Fig. 1.14

*(a) The robot's stick diagram on* $\lambda = -8^{\circ}$ *, Fixed ZMP,* $H_{\min} = 0.60m, H_{\max} = 0.62m$

*(b) The fixed ZMP diagram in nominal gait which satisfies stability criteria*

*(c) __: Shank M.C velocity, --: Tight M.C velocity*

*(d)__: Shank M.C acceleration, --:Tight M.C acceleration*

*(e) __: Shank angular velocity, --: Tight angular velocity*

*(f) __: Shank angular acceleration, --: Tight angular acceleration*

*(j) __: Shank M.C inertial force, --: Tight M.C inertial force*

*(h) __: Ankle joint torque, --: Hip joint torque, …: Shank joint torque*

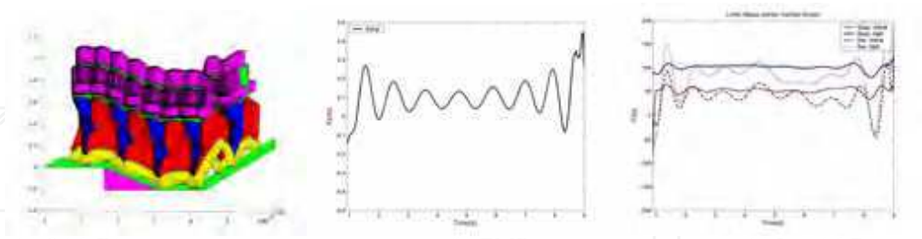

*(a) Stick Diagram* *(b) ZMP* *(c) Inertial Forces*

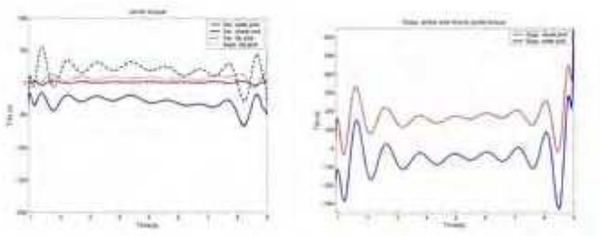

*(d) Driver Torques* *(e) Driver Torques*

Fig. 1.15 *(a) The robot's stick diagram on combined surface, nominal motion, Moving ZMP,* $\lambda = -8^{\circ}$ *(b) The moving ZMP diagram in nominal gait which satisfies stability criteria (c) Inertial forces: __: Supp. tight, --: Supp. shank, ….: Swing tight, .-: Swing shank (d) Joint's torques: __: Swing shank joint, --: Swing ankle joint, ….: Supp. hip joint, .-: Swing hip joint (e) Joint's torques: __: Supp. ankle joint, --: Supp. shank joint*

## 5. References


Peiman Naseradin Mousavi, Ahmad Bagheri, "*Mathematical Simulation of a Seven Link Biped Robot and ZMP Considerations*", Applied Mathematical Modelling, Elsevier, 2007, Vol. 31/1.

Q. Huang, K. Yokoi, S. Kajita, K. Kaneko, H. Arai, N. Koyachi, K. Tanie, "Planning Walking Patterns For A Biped Robot", IEEE Transactions on Robotics and Automation, VOL 17, No. 3, June 2001.

John J. G, "Introduction to Robotics: Mechanics and Control", Addison-Wesley, 1989.

H. K. Lum, M. Zribi, Y. C. Soh, " Planning and Contact of a Biped Robot", International Journal of Engineering Science 37(1999), pp. 1319-1349

Eric R. Westervelt, " Toward a Coherent Framework for the Control of Plannar Biped Locomotion", A dissertation submitted in partial fulfillment of the requirements for the degree of Doctor of Philosophy, (Electrical Engineering Systems), In the University of Michigan, 2003.

H. Hon, T. Kim, and T.Park, "Tolerance Analysis of a Spur Gear Train," in Proc. 3rd DADS Korean user's Conf. 1978, pp. 61-81

Peiman Naseradin. Mousavi, "Adaptive Control of 5 DOF Biped Robot Moving On A Declined Surface", M.S Thesis, Guilan University, 2006.

A. Bagheri, M.E. Felezi, P. N. Mousavi, " Adaptivr Control and Simulation of a Seven Link Biped Robot for the Combined Trajectory Motion and Stability Investigations", WSEAS Transactions on Systems, Issue 5, Vol. 5, May 2006, pp: 1214-1222

A. Bagheri. F. Najafi, R. Farrokhi, R. Y. Moghaddam, and M. E. Felezi, "Design, Dynamic Modification, and Adaptive Control of a New Biped Walking Robot", International Journal of Humanoid Robotics, Vol. 3, Num.1, March 2006, pp 105-126


**Humanoid Robots: New Developments**

Edited by Armando Carlos de Pina Filho

ISBN 978-3-902613-00-4

Hard cover, 582 pages

**Publisher** I-Tech Education and Publishing

**Published online** 01, June, 2007

**Published in print edition** June, 2007

For many years, the human being has been trying, in all ways, to recreate the complex mechanisms that form the human body. Such task is extremely complicated and the results are not totally satisfactory. However, with increasing technological advances based on theoretical and experimental researches, man gets, in a way, to copy or to imitate some systems of the human body. These researches not only intended to create humanoid robots, great part of them constituting autonomous systems, but also, in some way, to offer a higher knowledge of the systems that form the human body, objectifying possible applications in the technology of rehabilitation of human beings, gathering in a whole studies related not only to Robotics, but also to Biomechanics, Biomimmetics, Cybernetics, among other areas. This book presents a series of researches inspired by this ideal, carried through by various researchers worldwide, looking for to analyze and to discuss diverse subjects related to humanoid robots. The presented contributions explore aspects about robotic hands, learning, language, vision and locomotion.



**InTech Europe**

University Campus STeP Ri
Slavka Krautzeka 83/A
51000 Rijeka, Croatia
Phone: +385 (51) 770 447
Fax: +385 (51) 686 166
www.intechopen.com

**InTech China**

Unit 405, Office Block, Hotel Equatorial Shanghai
No.65, Yan An Road (West), Shanghai, 200040, China
中国上海市延安西路65号上海国际贵都大饭店办公楼405单元
Phone: +86-21-62489820
Fax: +86-21-62489821

IntechOpen